PROGRESS IN COMPENSATING PULSE SEQUENCES FOR QUANTUM COMPUTATION

J. TRUE MERRILL and KENNETH R. BROWN

School of Chemistry and Biochemistry, School of Computational Science and Engineering, School of Physics, Georgia Institute of Technology, Ford Environmental Science and Technology Building, 311 Ferst Dr, Atlanta, GA 30332-0400, USA

Advances in Chemical Physics, Volume 154: Quantum Information and Computation for Chemistry, First Edition. Edited by Sabre Kais.

I. INTRODUCTION

In any experiment, external noise sources and control errors limit the accuracy of the preparation and manipulation of quantum states. In quantum computing, these effects place an important fundamental limit on the size and accuracy of quantum processors. These restrictions may be reduced by quantum error correction. Although sophisticated quantum error-correcting codes are robust against any general error, these codes require large-scale multipartite entanglement and are especially challenging to implement in practice [1]. Therefore, it is of great interest to investigate schemes that reduce errors with a smaller resource overhead. One alternative strategy involves replacing an error-prone operation by a pulse sequence that is robust against the error.

The basis of our strategy is that all noises and errors can be treated as an unwanted dynamic generated by an error Hamiltonian. This error Hamiltonian can arise either through interactions with the environment or by the misapplication of control fields. This view unifies the pulse sequences developed for combating unwanted interactions (e.g., dynamic decoupling and dynamically corrected gates [2–4]), with those for overcoming systematic control errors, compensating composite pulse sequences [5]. In each case, the methods are limited by the rate at which control occurs relative to the time scale over which the error Hamiltonian fluctuates. However, many experiments are limited by control errors and external fields that vary slowly relative to the time scale of a single experimental run but vary substantially over the number of experiments required to obtain precise results.

In this chapter, we examine a number of techniques for handling unwanted control errors, including amplitude errors, timing errors, and frequency errors in the control field. We emphasize the common principles used to develop compensating pulse sequences and provide a framework in which to develop new sequences,

which will be of use to both quantum computation and coherent atomic and molecular spectroscopy.

II. COHERENT CONTROL OVER SPIN SYSTEMS

The accurate control of quantum systems is an important prerequisite for many applications in precision spectroscopy and in quantum computation. In complex experiments, the task reduces to applying a desired unitary evolution using a finite set of controls, which may be constrained by the physical limitations of the experimental apparatus. Stimulated by practical utility, quantum control theory has become an active and diverse area of research [6–10]. Although originally developed using nuclear-magnetic resonance (NMR) formalism, compensating pulse sequences can be approached from the perspective of quantum control theory with unknown systematic errors in the controls [11]. Here, we review several fundamental concepts in quantum control and apply these ideas using NMR as an instructive example. Although we restrict the discussion to control in NMR spectroscopy, the following analysis is quite general as several other coherent systems (e.g., semiconductor quantum dots [12], superconducting qubits [13–15], and trapped ions [16,17]) may be considered by minor modifications to the Hamiltonian.

In practice, a desired evolution is prepared by carefully manipulating the coupling of the system to a control apparatus, such as a spectrometer. In the absence of relaxation, the coherent dynamics are governed by the quantum propagator $U(t)$, which in nonrelativistic quantum mechanics must satisfy an operational Schrödinger equation:

$$\dot{U}(t) = -\mathrm{i}\left(\sum_{\mu} u_{\mu}(t) H_{\mu}\right) U(t), \qquad U(0) = \mathbb{1} \tag{1}$$

In this model, the unitless Hamiltonians $H_{\mu} \in \{H_1, H_2, \ldots, H_n\}$ are modulated by real-valued control functions $u_{\mu}(t) \in \{u_1(t), u_2(t), \ldots, u_n(t)\}$ and represent the n available degrees of control for a particular experimental apparatus. In analogy with linear vector spaces, we interpret the vector $\boldsymbol{u}(t) = (u_1(t), u_2(t), \ldots, u_n(t))$ as a vector function over the manifold of control parameters, with components $u_{\mu}(t)$ representing the magnitudes of the control Hamiltonians with units of angular frequency. It is convenient to introduce a second vector of control Hamiltonians $\boldsymbol{H} = (H_1, H_1, \ldots, H_n)$ and the short-hand notation $H(t) = \boldsymbol{u}(t) \cdot \boldsymbol{H}$. We omit a term that represents the portion of the total Hamiltonian outside direct control (i.e., a drift Hamiltonian); in principle it is always possible to work in an interaction picture where this term is removed. Alternatively, one may assign a Hamiltonian H_0 to represent this interaction, with the understanding that $u_0(t) = 1$ for all t.

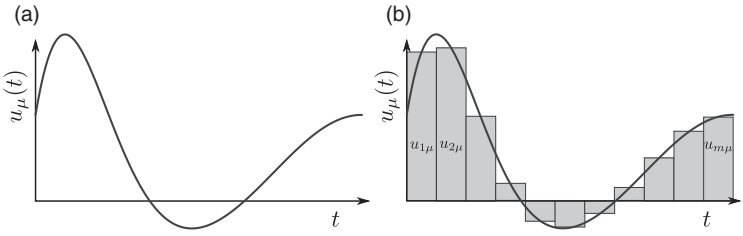

Figure 1. The experimental controls available to manipulate a quantum system are modeled using a set of real-valued control functions $\{u_\mu(t)\}$ that modify a set of dimensionless Hamiltonians $\{H_\mu\}$. (**a**) An example control function $u_\mu(t)$. (**b**) A discrete approximation for $u_\mu(t)$ composed of square pulses.

For a given control system, a natural question concerns the optimal approximation of a desired unitary propagation using a set of constrained control functions. Constraints may include limitations on the total operation length, control amplitudes, or derivatives. The study of this question requires the solution of Eq. (1) for a particular set of controls; such solutions may be obtained using several methods, including the Dyson series [18], and the Magnus [19,20], Fer [21], and Wilcox [22] expansions. We label particular solutions to the control equation over the interval $t_i \leq t \leq t_f$ as $U(\boldsymbol{u}(t); t_f, t_i)$. If the set of all possible solutions to Eq. (1) is the set of all unitary gates on the Hilbert space (i.e., the solutions form a representation of $\mathsf{U}(n)$ or $\mathsf{SU}(n)$, to be discussed in Section III.A) then the system is *operator controllable* [10,23].

For some applications, it is convenient to assume that the operation time τ is discretized into m-many time intervals, over which the control functions u_μ are constant; that is, during the kth time interval Δt_k the Hamiltonian is time-independent and the resulting evolution operator is $U_k = U(\boldsymbol{u}_k; t_k + \Delta t_k, t_k) = \exp(-\mathrm{i}\Delta t_k \boldsymbol{u}_k \cdot \boldsymbol{H})$. Figure 1 illustrates an example control function and a possible discretization scheme. Over each time interval, the applied unitary operation is a square pulse. In many experiments, the application of gates using sequences of square pulses is preferred for simplicity. The discretization of the control functions into square pulses allows one to solve Eq. (1) in a piecewise fashion. The total propagator for a sequence of m-many time-steps is given by the time-ordered product

$$U(\boldsymbol{u}(t), \tau, 0) = U_m U_{m-1} \ldots U_k \ldots U_2 U_1 = \prod_{k=1}^{m} U_k \tag{2}$$

where the differentiable multiplication of each successive operator is understood to be taken on the left; this is in agreement with standard quantum mechanics conventions, where operations are ordered right-to-left, but at odds with some

NMR literature where successive operations are ordered left-to-right. Frequently, we will consider propagators over the entire duration of a sequence $0 \leq t \leq \tau$; as a matter of notational convenience we drop the time interval labels whenever there is no risk of confusion. If a pulse sequence $U(\boldsymbol{u}(t))$ is equivalent to a target operation U_T in the sense that during an experiment, $U(\boldsymbol{u}(t))$ may be substituted for U_T, then $U(\boldsymbol{u}(t))$ is a *composite pulse sequence* [24,25].

The usefulness of composite pulse sequences lies in that in many cases, one may simulate a target unitary transformation U_T, which may be difficult to directly implement, by instead implementing a sequence of simpler pulses that under some set of conditions is equivalent to U_T. Composite pulse sequences may be designed to have several important advantages over a directly applied unitary, such as improved resilience to errors. The properties of pulses or pulse sequences may be considered either by the transformations produced on a particular initial state ρ, or by comparing the sequence to an ideal operation, which contains information on how the sequence transforms all initial states. Following Levitt [5], we assign composite pulses into two classes: the fully compensating class A, and the partially compensating class B. The properties of these classes are briefly reviewed.

Class A: All composite pulse sequences in class A may be written in the form

$$e^{i\phi} U(\boldsymbol{u}(t)) = U_T \tag{3}$$

where it is assumed that the individual pulses in the sequence are error-free. The global phase ϕ is irrelevant to the dynamics; for any initial state ρ, both the pulse sequence and the target operation apply the same transformation $(U(\boldsymbol{u}(t))\rho U^{\dagger}(\boldsymbol{u}(t)) = U_T \rho U_T^{\dagger})$. Sequences in this class are suited for use in quantum computation, because the transformation is independent of the initial quantum state. The study of these sequences will be the primary topic of this article.

Class B: Composite pulse sequences in class B transform one particular initial condition to a set of final conditions, which for the purposes of the experiment, are equivalent. For example, consider an NMR experiment on a spin $I = 1/2$ nucleus where the nuclear magnetization, initially oriented "spin-up" (i.e., $\rho = \mathbb{1}/2 + H_z$, where H_x, H_y, H_z are the nuclear angular momentum operators) is transferred to the H_x–H_y plane by a pulse sequence. In this sense, all sequences that apply the transformations are equivalent up to a similarity transform $\exp(-i\beta H_z)$, which applies a H_z phase to the spin. Other sequences in class B may satisfy $U(\boldsymbol{u}(t))\rho U^{\dagger}(\boldsymbol{u}(t)) = U_T \rho U_T^{\dagger}$ for a particular initial state ρ, but fail to satisfy Eq. (3). All sequences in class B are generally not well suited for use in quantum computation, because implementation requires specific knowledge of the initial and final states of the qubit register. Class B sequences are however useful in other applications, including NMR [24–26], MRI [27], control over nitrogen vacancy centers [28], and in ion trapping experiments [29]. We close our discussion by

noting that class B sequences may be converted into a fully compensating class A sequence by a certain symmetrical construction [30].

A. Errors in Quantum Control

We now consider the effects of unknown errors in the control functions. Recall that a pulse sequence may be specified by a set of control functions $\{u_\mu(t)\}$, which we group into a control vector $\boldsymbol{u}(t)$. Suppose, however, during an experiment an unknown systematic error deforms each of the applied controls from $u_\mu(t)$ to $v_\mu(t)$. In the presence of unknown errors, the perfect propagators $U(\boldsymbol{u}(t); t_f, t_i)$ are replaced with their imperfect counterparts $V(\boldsymbol{u}(t); t_f, t_i) = U(\boldsymbol{v}(t); t_f, t_i)$, which may be regarded as an image of the perfect propagator under the deformation of the controls.

In practice, systematic errors typically arise from a miscalibration of the experimental system, for example, an imprecise measurement of the intensity or frequency of a controlling field. In these cases, it is appropriate to introduce a deterministic model for the control deformation. Specifically, $\boldsymbol{v}(t)$ must be a function of the controls $\boldsymbol{u}(t)$, and for each component of the imperfect control vector we may write

$$v_\mu(t) = f_\mu[\boldsymbol{u}(t); \epsilon] \tag{4}$$

where the differentiable functional f_μ is the *error model* for the control and the variable ϵ is an unknown real parameter that parametrizes the magnitude of the error. This construction may be generalized to the case of multiple systematic errors by considering error models of the form $f_\mu[\boldsymbol{u}(t); \epsilon_i, \epsilon_j, \ldots, \epsilon_k]$. The model f_μ is set by the physics of the problem, and is chosen to produce the correct evolution under the imperfect controls. Formally, we may perform the expansion

$$f_\mu[\boldsymbol{u}(t); \epsilon] = f_\mu[\boldsymbol{u}(t); 0] + \epsilon \frac{d}{d\epsilon} f_\mu[\boldsymbol{u}(t); 0] + \frac{\epsilon^2}{2!} \frac{d^2}{d\epsilon^2} f_\mu[\boldsymbol{u}(t); 0] + \mathcal{O}(\epsilon^3) \tag{5}$$

then by the condition that when $\epsilon = 0$ the control must be error free, it is trivial to identify $u_\mu(t) = f_\mu[\boldsymbol{u}(t); 0]$. Frequently, it is sufficient to consider models that are linear in the parameter ϵ. In this case, we introduce the shorthand notation $\delta u_\mu(t) = \frac{d}{d\epsilon} f_\mu[\boldsymbol{u}(t); 0]$ and the corresponding vector $\boldsymbol{\delta u}(t)$ to represent the first-order deformation of the controls, so that the imperfect controls take the form $v_\mu(t) = u_\mu(t) + \epsilon \delta u_\mu(t)$. Figure 2 illustrates two common error models: constant offsets from the ideal control value ($f_\mu[\boldsymbol{u}(t); \epsilon] = u_\mu(t) + \epsilon$), and errors in the control amplitude ($f_\mu[\boldsymbol{u}(t); \epsilon] = (1 + \epsilon) u_\mu(t)$).

A natural question to ask is what effect unknown errors have on the evolution of the system. It is obvious that imperfect pulses make accurate manipulation of a quantum state difficult. One may be surprised to find that for some cases, the effects

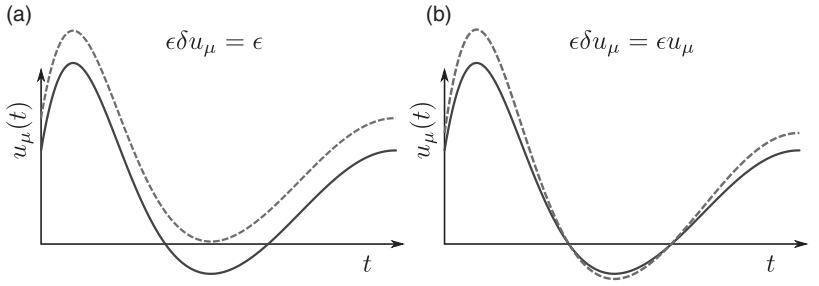

Figure 2. Systematic errors induce deformations of the ideal control functions $u_\mu(t)$ (solid curves) to the imperfect controls $v_\mu(t) = u_\mu(t) + \epsilon\delta u_\mu(t)$ (dashed curves). Common error models include (**a**) a constant unknown offset in the control and (**b**) an error in the amplitude of the control function.

of errors on the controls may be systematically removed, without knowledge of the amplitude ϵ. The method we describe involves implementing a compensating composite pulse sequence that is robust against distortion of the controls by a particular error model. As an example, consider a case where an experimentalist would like to approximate a target unitary $U_T = U(\boldsymbol{u}(t); \tau, 0)$, where at least one of the controls is influenced by a systematic error. The target operation may be simulated up to $\mathcal{O}(\epsilon^n)$ if a set of control functions $\boldsymbol{u}(t)$ exists such that

$$V(\boldsymbol{u}(t); \tau, 0) = U(\boldsymbol{u}(t) + \epsilon\boldsymbol{\delta u}(t); \tau, 0) = U(\boldsymbol{u}(t); \tau, 0) + \mathcal{O}(\epsilon^{n+1}) \tag{6}$$

Many (infinite in most cases) sets of control functions $\boldsymbol{u}(t)$ implement a target unitary transformation, however, only a small subset of possible control functions are robust to distortion by a particular systematic error. If robust controls can be found, then pulse sequence $V(\boldsymbol{u}(t); \tau, 0)$ can be applied in the place of U_T, and the leading order terms of the offset $\epsilon\boldsymbol{\delta u}(t)$ are suppressed. A sequence with these properties is called a *compensating pulse sequence*, and may be thought of as a set of control functions that are optimized to remove the effect of leading-order terms of unknown systematic errors in the controls. By construction, sequences of this form are fully compensating (Class A).

When an experimentalist implements a compensating pulse sequence they attempt to apply the ideal operations $U(\boldsymbol{u}(t); \tau, 0)$, ignorant of the amplitude ϵ of a systematic error. However, the operations are not ideal and to emphasize this we introduce $V(\boldsymbol{u}(t); \tau, 0)$ to represent the *imperfect propagators* that are actually implemented when $U(\boldsymbol{u}(t); \tau, 0)$ is attempted. The functional dependence of the error in $V(\boldsymbol{u}(t); \tau, 0)$ is not explicitly written, allowing us to study different error models with the same pulse sequence.

Let us consider the dynamics of the system under the interaction frame Hamiltonian $H^I(t) = \sum_\mu \epsilon\delta u_\mu(t) H^I_\mu(t)$, where $H^I_\mu(t) = U^\dagger(\boldsymbol{u}(t'); t, 0) H_\mu U(\boldsymbol{u}(t'); t, 0)$

are the control Hamiltonians in the interaction frame. In this picture, $H^I(t)$ is regarded as a perturbation, and we associate the propagator $U^I(\boldsymbol{\delta u}(t); \tau, 0)$ as the particular solution to the interaction picture Schrödinger equation over the interval $0 \leq t \leq \tau$. Hence,

$$V(\boldsymbol{u}(t); \tau, 0) = U(\boldsymbol{u}(t); \tau, 0) U^I(\epsilon \boldsymbol{\delta u}(t); \tau, 0) \tag{7}$$

and from Eq. (6)

$$U^I(\epsilon \boldsymbol{\delta u}(t); \tau, 0) = \mathbb{1} + \mathcal{O}(\epsilon^{n+1}) \tag{8}$$

Quite generally, when a fully compensating pulse sequence is transformed into the interaction frame the resulting propagator must approximate the identity operation [31]. The techniques for constructing compensating pulse sequences discussed in the present chapter rely on performing a series expansion by powers of ϵ for the interaction frame propagator $U^I(\epsilon \boldsymbol{\delta u}(t); \tau, 0)$, then choosing a set of controls that remove the leading terms of the distortion, and finally transforming back out of the interaction frame.

B. NMR Spectroscopy as a Model Control System

In this section, we will apply the ideas developed thus far to a model one-qubit NMR quantum computer [32,33], which serves as a relevant example of a system where coherent control is possible. In Section V.A, multi qubit operations are considered. The many possible physical implementations for a qubit are often based on a two-level subsystem of a larger Hilbert space. In this case, the qubit is defined on the angular momentum states of a spin-1/2 nucleus.

Consider an ensemble of spin $I = 1/2$ nuclei undergoing Larmor precession under a static magnetic field $\boldsymbol{B}_0$ oriented along the $\hat{\mathbf{z}}$ axis. The static field $\boldsymbol{B}_0$ induces a net magnetization among the nuclei. A transverse radiofrequency (rf) field near nuclear resonance $\boldsymbol{B}_1(t) = \boldsymbol{B}_1 \cos(\omega_1 t - \phi)$ is applied in the $\hat{\mathbf{x}}$–$\hat{\mathbf{y}}$ plane. A simplified diagram of an NMR spectrometer is provided in Fig. 3. The analysis is simplified by assuming that individual nuclei in the ensemble are decoupled by

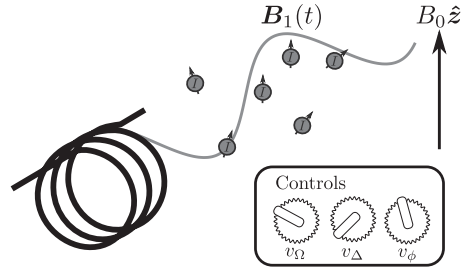

Figure 3. Simplified diagram of an NMR spectrometer. Control over an ensemble of nuclear spins is applied by a radiofrequency (rf) field $\boldsymbol{B}_1(t)$, where the Rabi frequency $\Omega(t)$, field detuning $\Delta(t)$, and phase $\phi(t)$ are control parameters. Unknown systematic control errors (e.g., poor intensity control, detuning errors) may be present.

the rapid tumbling of spins in the sample [25]. After transforming into the rotating frame, the Hamiltonian for a single spin may be written as

$$H(t) = \Delta(t)H_z + \Omega(t)\big(\cos(\phi(t))H_x + \sin(\phi(t))H_y\big) \tag{9}$$

where

$$H_x = \frac{1}{2}\begin{pmatrix} 0 & 1 \\ 1 & 0 \end{pmatrix}, \qquad H_y = \frac{1}{2}\begin{pmatrix} 0 & -i \\ i & 0 \end{pmatrix}, \qquad H_z = \frac{1}{2}\begin{pmatrix} 1 & 0 \\ 0 & -1 \end{pmatrix}$$

and the counter-rotating terms have been neglected under the rotating-wave approximation. Manipulation of the rf field provides a convenient set of controls to guide the evolution of the spins; it is assumed that the rf field detuning $\Delta(t)$, phase $\phi(t)$, and the Rabi frequency $\Omega(t)$ are each independently controllable and may suffer from independent systematic errors. Let the controls $\boldsymbol{u}(t)$ denote the vector $(\Omega(t)\cos(\phi(t)), \Omega(t)\sin(\phi(t)), \Delta(t))$. Then the Hamiltonian may be written as $H(t) = \boldsymbol{u}(t) \cdot \boldsymbol{H}$, and the resulting Schrödinger equation for the propagator is of the form of Eq. (1). Thus, the coherent spin dynamics in magnetic resonance spectroscopy can be reformulated in terms of a problem in quantum control.

1. *Error Models*

In practice, systematic errors in the controls caused by instrumental limitations prohibit the application of perfect pulse propagators. We consider several models for errors in the controls of a one-qubit NMR quantum computer. Often compensating pulse sequences are well optimized for one type of error, but provide no advantage against a different error model.

a. Amplitude Errors. An amplitude error arises from slow systematic variation in the amplitude of the rf field, resulting in a small offset in the applied Rabi frequency. Let Ω represent the ideal Rabi frequency and Ω' represent the offset. From the form of the control vector $\boldsymbol{u}(t)$ it follows that in the presence of the error, the $u_x(t)$ and $u_y(t)$ controls are distorted; that is, they are replaced by their imperfect counterparts $v_{x/y}(t) = u_{x/y}(t) + \epsilon_A \delta u_{x/y}(t)$, where $\delta u_{x/y}(t) = u_{x/y}(t)$ is proportional to the ideal control value, and the error parameter $\epsilon_A = \Omega'/\Omega < 1$ is the relative amplitude of the field offset. The imperfect pulses take the form $V(\boldsymbol{u}(t)) = U(\boldsymbol{u}(t)(1 + \epsilon_A))$.

b. Pulse Length Errors. A pulse length error is a systematic error in the duration of individual pulses, perhaps due to an offset in the reference oscillator frequency. The imperfect propagator takes the form $V(\boldsymbol{u}(t); t_0 + \Delta t, t_0) = U(\boldsymbol{u}(t); t_0 + \Delta t + \delta t, t_0)$, where Δt is the ideal pulse length and δt is the unknown timing error. In some cases, errors on the clock may be rewritten in terms of equivalent errors on

the control functions. For simplicity, we restrict ourselves to square pulses, where the controls $\boldsymbol{u}(t)$ are constant and the imperfect propagator may be rewritten as $V(\boldsymbol{u}; t_f, t_i) = U(\boldsymbol{u} + \epsilon_T \boldsymbol{\delta u}; t_0 + \Delta t, t_0)$, where again $\boldsymbol{\delta u} = \boldsymbol{u}$ is proportional to the ideal control and now $\epsilon_T = \delta t / \Delta t$, similar to the result for an amplitude error. Amplitude and pulse length errors in square pulses are similar in some senses; although they arise from distinct physical processes, they both act as errors in the angle of the applied rotation.

c. Addressing Errors. Individual spins among the ensemble may experience slightly different Rabi couplings owing to the spatial variation in the strength of the control field. In some applications this variation is exploited to yield spatially localized coherent operations, such as in magnetic resonance imaging, and in addressing single atoms in optical lattices or single ions in ion trap experiments [17,34]. In fact, many proposed scalable architectures for quantum processors rely on this effect to discriminate between qubits. In these cases, it is important to distinguish between the evolution applied to the addressed spins and the evolution of spins outside of the addressed region, where ideally no operation is applied.

Consider an experiment where the ensemble of spins is divided into a high field, Ω, and low field, $\Omega' < \Omega$, region. We assume that the control of the addressed (high-field) spins is perfect (i.e., for addressed spins $V(\boldsymbol{u}(t)) = U(\boldsymbol{u}(t))$); however, the spins in the low-field region experience an undesired correlated rotation $V(\boldsymbol{u}(t)) = U(\epsilon_N \boldsymbol{u}(t))$, where $\epsilon_N = \Omega' / \Omega$ (the subscript N denotes neighboring spins). In many cases, the imperfect pulses on the unaddressed qubits may be regarded as very small rotations. From a mathematical point of view, sequences composed of these rotations are more easily attacked using the expansion techniques that will be developed in Section III.B.

d. Detuning Errors. Systematic errors may also arise in the control of the frequency of the rf field. Consider the case where an experimentalist attempts to perform an operation at a particular field tuning $\Delta(t)$, however, a slow unknown frequency drift $\delta(t)$ is present. From the form of the NMR controls, it follows that the error distorts the H_z component to $v_z(t) = u_z(t) + \epsilon_D \delta u_z$, where $u_z = \Delta(t)$, and $\epsilon_D \delta u_z(t) = \delta(t)$. Unlike the other models discussed thus far, the detuning error applies a shift in the effective rotation axis, rotating it in the direction of the H_z axis. Therefore, the ideal propagator and the imperfect counterpart do not commute in general.

C. Binary Operations on Unitary Operators

In our discussion of the properties of compensating pulse sequences, it will be necessary to study the structure of the control Hamiltonians $\{H_\mu\}$, and to calculate

the accuracy of gates. Here, we discuss the Hilbert–Schmidt product and the fidelity measure.

1. *Hilbert–Schmidt Inner Product*

The Hilbert–Schmidt inner product (also known as the Frobenius product) is a natural extension of the vector inner product over the field of complex numbers to matrices with complex coefficients. Let U and V be $n \times n$ matrices with entries U_{ij} and V_{ij}, respectively. The Hilbert–Schmidt inner product $\langle U, V\rangle$ is defined as

$$\langle U, V\rangle = \sum_{i=1}^{n}\sum_{j=1}^{n} U_{ji}^{*} V_{ij} = \mathrm{tr}(U^{\dagger} V) \tag{10}$$

This inner product has several properties that closely mirror the inner product for complex vectors, namely $\langle U, V\rangle = \langle V, U\rangle^{*}$, and $|\langle U, V\rangle| \leq ||U||_{\mathrm{HS}}\, ||V||_{\mathrm{HS}}$, where the Hilbert–Schmidt norm $||U||_{\mathrm{HS}} = \sqrt{\langle U, U\rangle}$ also satisfies a corresponding triangle inequality $||U + V||_{\mathrm{HS}} \leq ||U||_{\mathrm{HS}} + ||V||_{\mathrm{HS}}$. This strong correspondence to Euclidean vector spaces will be exploited in the next section, where Lie-algebraic techniques are employed to construct compensating pulse sequences.

2. *Fidelity*

A useful measure for evaluating the effects of a systematic control error is the operational fidelity, defined as

$$\mathcal{F}(U, V) = \min_{\psi} \sqrt{\langle\psi|U^{\dagger} V|\psi\rangle\langle\psi|V^{\dagger} U|\psi\rangle} \tag{11}$$

For any two unitary matrices in the group $\mathsf{SU}(2)$, the fidelity may be written as $\mathcal{F}(U, V) = |\langle U, V\rangle|/2$. In this chapter, we show error improvement graphically by plotting the infidelity, $1 - \mathcal{F}(U, V)$.

III. GROUP THEORETIC TECHNIQUES FOR SEQUENCE DESIGN

In the present work, we briefly discuss several aspects of the theory of Lie groups, which are useful for constructing compensating pulse sequences, with emphasis on conceptual clarity over mathematical rigor. The interested reader is referred to Refs [10] and [35] for additional details and a rigorous treatment of the subject. Quantum control theory and the related study of continuous transformation groups are rich and active subjects, with applications in chemistry [36–38], and other applications requiring the precise manipulation of quantum states [39,40]. We

turn our attention to continuous groups of quantum transformations, specifically transformations that induce qubit rotations in quantum computing.

A. Lie Groups and Algebras

Consider the family of unitary operators that are solutions to the control equation

$$\dot{U}(t) = \sum_{\mu} u_{\mu}(t)\tilde{H}_{\mu}U(t), \qquad U(0) = \mathbb{1} \tag{12}$$

where $\tilde{H}_{\mu} = -\mathrm{i}H_{\mu}$ are skew-symmetrized Hamiltonians with the added condition that the (possibly infinite) set of control Hamiltonians $\{\tilde{H}\}$ is closed under the commutation operation (in the sense that for all $\tilde{H}_{\mu}$, $\tilde{H}_{\nu} \in \{\tilde{H}\}$, $\alpha[\tilde{H}_{\mu}, \tilde{H}_{\nu}] \in \{\tilde{H}\}$, where $\alpha \in \mathbb{R}$). This extra condition does not exclude any of the "physical" solutions that are generated by a subset of $\{\tilde{H}\}$, because these operators correspond to solutions where the remaining control functions $u_{\mu}(t)$ have been set to zero. Observe that these solutions form a representation of a group, here denoted as G, because the following properties are satisfied: for all solutions U_1 and U_2, the product U_1U_2 is also a solution (see Section III.B); the associative property is preserved (i.e., $U_1(U_2U_3) = (U_1U_2)U_3$); the identity $\mathbb{1}$ is a valid solution; and for all solutions U_1, the inverse $U_1^{\dagger}$ is also a valid solution. Moreover, the group forms a continuous differentiable manifold, parametrized by the control functions. A continuous group that is also a differentiable manifold with analytic group multiplication and group inverse operations is called a *Lie group*. We identify the group G of solutions as a Lie group, and note that differentiation of the elements $U \in \mathsf{G}$ is well defined by nature of Eq. (12).

We now turn our attention to elements of G in the neighborhood of the identity element, that is, infinitesimal unitary operations. In analogy with differentiation on Euclidean spaces, note that for any $U(t) \in \mathsf{G}$ one may find a family of tangent curves at $U(0) = \mathbb{1}$,

$$\left.\frac{dU(t)}{dt}\right|_{t=0} = \sum_{\mu} u_{\mu}(0)\tilde{H}_{\mu} \tag{13}$$

The set of skew-symmetrized Hamiltonians $\{\tilde{H}\}$ and the field of real numbers $\mathbb{R}$ (corresponding to the allowed values for the components $u_{\mu}(0)$) form a linear vector space under matrix addition and the Hilbert–Schmidt inner product [35]. Here, the Hamiltonians $\tilde{H}$ take the place of Euclidean vectors and span the tangent space of G at the identity, denoted by $T_{\mathbb{1}}\mathsf{G}$. A homomorphism exists between the control functions $\boldsymbol{u}(0)$ and vectors in $T_{\mathbb{1}}\mathsf{G}$. On this space is defined the binary Lie bracket operation between two vectors $[\tilde{H}_{\mu}, \tilde{H}_{\nu}]$, which for our purposes is synonymous with the operator commutator. A vector space that is closed under the Lie bracket is an example of a *Lie algebra*. By construction, the set $\{\tilde{H}\}$ is

closed under commutation and therefore forms a Lie algebra, here denoted as $\mathfrak{g}$, corresponding to the Lie group G. We note that in general the Hamiltonians may be linearly dependent; however, an orthogonal basis under the Hilbert–Schmidt product may be generated using an orthogonalization algorithm.

The power of most Lie algebraic techniques relies on the mapping between group elements that act on a manifold (such as the manifold of rotations on a Bloch sphere) to elements in a Lie algebra, which are members of a vector space. In the groups we study here, the mapping is provided by the exponential function $\mathsf{G} = \mathrm{e}^{\mathfrak{g}}$ (i.e., every element $U \in \mathsf{G}$ may be written as $U = \mathrm{e}^{g}$ where $g \in \mathfrak{g}$). The object of this method is to study the properties of composite pulse sequences, which are products of members of a Lie group, in terms of vector operations on the associated Lie algebra.

1. The Spinor Rotation Group $\mathsf{SU}(2)$

As a relevant example, consider the group of single-qubit operations generated by the NMR Hamiltonian Eq. (9). This is a representation of the special unitary group $\mathsf{SU}(2)$. The skew-symmetrized control Hamiltonians are closed under the Lie bracket and thus form a representation of the Lie algebra $\mathfrak{su}(2) = \mathrm{span}\{-\mathrm{i}H_x, -\mathrm{i}H_y, -\mathrm{i}H_z\}$.[1] Therefore, any element in $U \in \mathsf{SU}(2)$ may be written as $U = \mathrm{e}^{-\mathrm{i}t\boldsymbol{u}\cdot\boldsymbol{H}}$, where $-\mathrm{i}t\boldsymbol{u} \cdot \boldsymbol{H} \in \mathfrak{su}(2)$ may now be interpreted as a vector on the the Lie algebra. Furthermore, since $\langle -\mathrm{i}H_\mu, -\mathrm{i}H_\nu \rangle = \delta_{\mu,\nu}/2$, the spin operators form an orthogonal basis for the algebra. Topologically $\mathsf{SU}(2)$ is compact and is homomorphic to rotations of the 2-sphere, the group $\mathsf{SO}(3)$ [35]; exactly two group elements, U and $-U \in \mathsf{SU}(2)$, map to the same rotation.

B. Baker–Campbell–Hausdorff and Magnus Formulas

A composite pulse sequence may be studied from the perspective of successive products between elements of a Lie group. In the following analysis, it will be useful to relate the product of two members of a Lie group to vector operations on the Lie algebra. The relationship allows us to map pulse sequences to effective Hamiltonians. This correspondence is provided by the Baker–Campbell–Hausdorff (BCH) formula [35,41], which relates group products to a series expansion in the Lie algebra. For rapid convergence, it is most convenient to consider products of infinitesimal unitary operations, that is, operations of the form $\mathrm{e}^{\epsilon g}$, where $g \in \mathfrak{g}$ and $\epsilon < 1$ is a real expansion parameter. We assume ϵ is sufficiently small to guarantee that the group product of propagators always lies within the radius of convergence for the expansion [20]. Let $U_1 = \mathrm{e}^{\epsilon \tilde{H}_1}$ and $U_2 = \mathrm{e}^{\epsilon \tilde{H}_2}$ be members of a Lie group G, where the Hamiltonians $\tilde{H}_1, \tilde{H}_2 \in \mathfrak{g}$ are members of the

[1] The operation span denotes all linear combinations with real coefficients

associated algebra. The BCH representation for the product $U_1 U_2 = U_3$ involves the calculation of an effective Hamiltonian $\tilde{H}_3 \in \mathfrak{g}$ by the expansion

$$U_3 = \exp(\tilde{H}_3) = \exp\left(\sum_n^{\infty} \epsilon^n F_n\right) \tag{14}$$

where the terms

$$\begin{aligned}
\epsilon F_1 &= \epsilon(\tilde{H}_1 + \tilde{H}_2) \\
\epsilon^2 F_2 &= \frac{\epsilon^2}{2}[\tilde{H}_1, \tilde{H}_2] \\
\epsilon^3 F_3 &= \frac{\epsilon^3}{12}\Big([\tilde{H}_1, [\tilde{H}_1, \tilde{H}_2]] + [\tilde{H}_2, [\tilde{H}_2, \tilde{H}_1]]\Big)
\end{aligned}$$

are calculated from $\tilde{H}_1, \tilde{H}_2$, and nested commutators of elements of the Lie algebra. A combinatoric formula found by Dykin [42] exists to calculate F_n for arbitrary n. The expansion may be truncated once a desired level of accuracy is reached. In principle, group products of any length may be approximated to arbitrary accuracy using BCH formulas; however, these formulas rapidly become unwieldy and difficult to use without the aid of a computer. The BCH expansion is most useful for sequences of square pulses, where for each pulse the Hamiltonian is time independent.

1. *The Magnus Expansion*

A related expansion developed by Magnus [19] may be used to compute the propagator generated by a general time-dependent Hamiltonian. The solution to a control equation (e.g., $\dot{U}(t) = \epsilon\tilde{H}(t)U(t)$, where $\epsilon\tilde{H}(t) = \sum_\mu \epsilon\delta u_\mu(t)\tilde{H}_\mu$) over the interval $t_i \le t \le t_f$ may be written as the power series

$$U(\epsilon\boldsymbol{\delta u}; t_f, t_i) = \exp\left(\sum_n^{\infty} \epsilon^n \Omega_n(t_f, t_i)\right) \tag{15}$$

where the first few expansion terms are

$$\begin{aligned}
\epsilon\Omega_1(t_f, t_i) &= \epsilon \int_{t_i}^{t_f} dt\tilde{H}(t) \\
\epsilon^2\Omega_2(t_f, t_i) &= \frac{\epsilon^2}{2}\int_{t_i}^{t_f} dt \int_{t_i}^{t} dt'[\tilde{H}(t), \tilde{H}(t')] \\
\epsilon^3\Omega_3(t_f, t_i) &= \frac{\epsilon^3}{6}\int_{t_i}^{t_f} dt \int_{t_i}^{t} dt' \int_{t_i}^{t'} dt''([\tilde{H}(t), [\tilde{H}(t'), \tilde{H}(t'')]] \\
&\quad + [\tilde{H}(t''), [\tilde{H}(t'), \tilde{H}(t)]])
\end{aligned}$$

Again as a matter of notational convenience, we drop the time interval labels (t_f, t_i) on the expansion terms when there is no risk of confusion. Formulas for higher-order terms may be found in Ref. [43]. The BCH and Magnus expansions are in fact intimately related; when considering piecewise-constant controls the techniques are equivalent. We refer the interested reader to Ref. [20] for further details regarding both the Magnus expansion and BCH formulas.

The BCH and Magnus expansions are well known in composite pulse literature, and techniques that utilize these expansions are collectively referred to as average Hamiltonian theory. A variant of this technique, pioneered by Waugh [44,45], has been a mainstay of composite pulse design in the NMR community for decades. In some formalisms, the BCH expansion of the product of two propagators is interpreted as a power series in the rotation axis and angle. For the study of composite single-qubit rotations, this picture is extremely useful as it allows rotations on the sphere to guide the mathematics. However, this picture of composite rotations cannot be generalized to more complex groups, such as the group of n-qubit operations $\mathsf{SU}(2^n)$.

In this work, we emphasize a Lie algebraic interpretation of these methods, which also leads to a second geometric picture for the terms of the expansions. Observe that the first-order terms F_1 and Ω_1 may be regarded as simple vector sums on the Lie algebra (i.e., the sum of $\tilde{H}_1$ and $\tilde{H}_2$ in the BCH expansion and the sum of each of the infinitesimal vectors $\tilde{H}(t)dt$ in the Magnus expansion). In an analogous way, one may interpret the higher-order terms as the addition of successively smaller vectors on $\mathfrak{g}$. From this insight, one may construct composite sequences that simulate a target unitary from geometric considerations on the Lie algebra.

2. *A Method for Studying Compensation Sequences*

At this point, it is useful to introduce the general method that will be used to study compensating pulse sequences. Recall from Section II.A that in the presence of an unknown systematic control error, the ideal control functions are deformed into imperfect analogues. The imperfect propagator may be decomposed as $V(\boldsymbol{u}(t); \tau, 0) = U(\boldsymbol{u}(t); \tau, 0)U^I(\epsilon\boldsymbol{\delta u}(t); \tau, 0)$, where $U^I(\epsilon\boldsymbol{\delta u}(t); \tau, 0)$ represents the portion of the evolution produced by the systematic distortion of the ideal controls. Provided that the displacements $\epsilon\boldsymbol{\delta u}(t)$ are sufficiently small relative to the ideal controls, we may perform a Magnus expansion for the interaction frame propagator

$$U^I(\epsilon\boldsymbol{\delta u}(t); \tau, 0) = \exp\left(\sum_{n=1}^{\infty} \epsilon^n \Omega_n(\tau, 0)\right) \tag{16}$$

where the integrations in the expansion terms are performed in the appropriate frame. For example, the first-order term is

$$\epsilon\Omega_1(\tau, 0) = -\mathrm{i}\epsilon \int_0^\tau dt\ \boldsymbol{\delta u}(t) \cdot \boldsymbol{H}^I(t) \tag{17}$$

where the components $H_\mu^I(t) = U^\dagger(\boldsymbol{u}(t'); t, 0) H_\mu U(\boldsymbol{u}(t'); t, 0)$ are the interaction frame control Hamiltonians. The reader should recall from Eq. (8) that if the controls $\boldsymbol{u}(t)$ form an nth order compensating pulse sequence, then the interaction frame propagator $U^I(\epsilon\boldsymbol{\delta u}(t); \tau, 0) = \mathbb{1} + \mathcal{O}(\epsilon^{n+1})$ must approximate the identity to sufficient accuracy. It immediately follows that this condition is satisfied for any ϵ when the leading n-many Magnus expansion terms $\Omega_1(\tau, 0), \Omega_2(\tau, 0), \ldots, \Omega_n(\tau, 0)$ over the pulse interval $0 \leq t \leq \tau$ simultaneously equal zero.

This condition may also be understood in terms of geometric properties of vector paths on the Lie algebra. For example, consider the first-order Magnus expansion term for the interaction frame propagator and observe that $-\mathrm{i}\epsilon\boldsymbol{\delta u}(t) \cdot \boldsymbol{H}^I(t)$ may be regarded as a vector path on the dynamical Lie algebra. From the condition $\Omega_1(\tau, 0) = 0$ and Eq. (17), we see that the path must form a closed cycle in order for the first-order term to be eliminated (see Fig. 4). The elimination of higher-order expansion terms will place additional geometric constraints on the path, which will depend on the structure of the Lie algebra (i.e., the commutators between paths on the algebra). In the case of piecewise constant control functions, the resulting propagator may be understood as a sequence of square pulses. It is clear that in this case the Magnus series reduces to a BCH expansion for the total pulse propagator, and on the Lie algebra the corresponding path forms a closed polygon.

This Lie theoretic method is a useful tool in determining whether a control function $\boldsymbol{u}(t)$ is also a compensating sequence; we may directly calculate the interaction frame Magnus expansion terms in a given error model and show that they equal zero. The inverse problem (i.e., solving for control functions) is typically much more difficult. In general, the interaction Hamiltonians $H_\mu^I(t)$ are highly nonlinear functions of the ideal controls $\boldsymbol{u}(t)$, which impedes several analytical

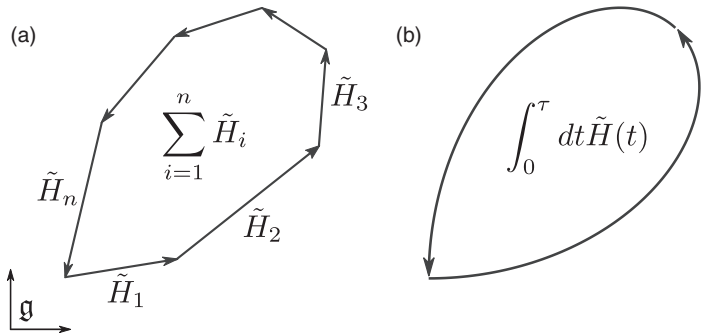

Figure 4. Vector paths on a Lie algebra $\mathfrak{g}$ may be used to represent a pulse sequence. (**a**) The BCH expansion relates group multiplication of several square pulses to vector addition on $\mathfrak{g}$. (**b**) A shaped pulse is represented by a vector curve on $\mathfrak{g}$, parametrically defined by the control functions. Both pulse sequences form a closed loop on $\mathfrak{g}$ and therefore the first-order terms equal zero.

solution methods. However, we note that in several special cases the problem is considerably simplified, such as when the ideal operation is to perform the identity, and the interaction and Schrödinger pictures are equivalent.

C. Decompositions and Approximation Methods

Several useful techniques in sequence design involve decompositions that may be understood in terms of the structure of a Lie group and its corresponding algebra. In this section, we discuss several important methods and identities.

1. *Basic Building Operations*

Given a limited set of controls $\{\tilde{H}_1, \tilde{H}_2\}$ that generate the algebra $\mathfrak{g}$, one may produce any unitary operation in the corresponding Lie group $\mathsf{G} = \mathrm{e}^{\mathfrak{g}}$ using only two identities. The first identity, the Lie–Trotter formula [46], describes how to produce a unitary generated by the sum of two noncommuting control operators. Using the BCH formula one may compute that $\mathrm{e}^{\tilde{H}_1/n}\mathrm{e}^{\tilde{H}_2/n} = \mathrm{e}^{(\tilde{H}_1+\tilde{H}_2)/n} + \mathcal{O}([\tilde{H}_1, \tilde{H}_2]/n^2)$. In terms of physical pulses, this corresponds to dividing the propagators $\mathrm{e}^{\tilde{H}_1}$ and $\mathrm{e}^{\tilde{H}_2}$ into n equal intervals to produce the propagators $\mathrm{e}^{\tilde{H}_1/n}$ and $\mathrm{e}^{\tilde{H}_2/n}$. Suppose we perform n such successive products, so that the resulting propagator is

$$\left(\mathrm{e}^{\tilde{H}_1/n}\mathrm{e}^{\tilde{H}_2/n}\right)^n = \mathrm{e}^{\tilde{H}_1+\tilde{H}_2} + \mathcal{O}([\tilde{H}_1, \tilde{H}_2]/n) \tag{18}$$

Although the Hamiltonians $\tilde{H}_1$ and $\tilde{H}_2$ do not commute in general, we may approximate $U = e^{\tilde{H}_1+\tilde{H}_2}$ to arbitrary accuracy by dividing the evolution into n-many time intervals and using the construction Eq. (18). By extension, it follows that any unitary generated by a Hamiltonian in the Lie algebra subspace $\mathrm{span}\{\tilde{H}_1, \tilde{H}_2\}$ may be approximated to arbitrary accuracy using a Trotter sequence. A number of improved sequences were developed by Suzuki [47] that remove errors to higher commutators and scale more strongly with n. The Trotter-Suzuki formulas may be used to eliminate successively higher-order errors at the cost of increased operation time [48].

The second identity, which we refer to as the balanced group commutator, enables the synthesis of a unitary generated by the Lie bracket $[\tilde{H}_1, \tilde{H}_2]$. Again the BCH formula may be used to show $\mathrm{e}^{\tilde{H}_1/n}\mathrm{e}^{\tilde{H}_2/n}\mathrm{e}^{-\tilde{H}_1/n}\mathrm{e}^{-\tilde{H}_2/n} = \mathrm{e}^{[\tilde{H}_1,\tilde{H}_2]/n^2} + \mathcal{O}([\tilde{H}_1 + \tilde{H}_2, [\tilde{H}_1, \tilde{H}_2]]/n^3)$. If we now consider n^2-many successive balanced group commutator constructions, the resulting propagator is

$$\left(\mathrm{e}^{\tilde{H}_1/n}\mathrm{e}^{\tilde{H}_2/n}\mathrm{e}^{-\tilde{H}_1/n}\mathrm{e}^{-\tilde{H}_2/n}\right)^{n^2} = \mathrm{e}^{[\tilde{H}_1,\tilde{H}_2]} + \mathcal{O}([\tilde{H}_1 + \tilde{H}_2, [\tilde{H}_1, \tilde{H}_2]]/n) \tag{19}$$

Then, as in the case of the Trotter formula, we may approximate $U = \mathrm{e}^{[\tilde{H}_1,\tilde{H}_2]}$ to arbitrary accuracy by increasing the number of intervals n. By assumption the entire

Lie algebra may be generated by nested Lie brackets between the Hamiltonians $\tilde{H}_1$ and $\tilde{H}_2$, which implies that any $U \in \mathsf{G}$ may be produced by a combination of balanced group commutator and Trotter formulas. However, we emphasize that in almost all cases much more efficient constructions exist. The balanced group commutator construction also forms the basis of the Solovay-Kitaev theorem [49], an important result regarding the universality of a finite gate set in quantum computation. Later, we will study the Solovay-Kitaev method (see Section IV.A.1), which produces compensating sequences of arbitrary accuracy by using a balanced group commutator. Specifically we will use the formula

$$\exp(\tilde{H}_1\epsilon^k)\exp(\tilde{H}_2\epsilon^l)\exp(-\tilde{H}_1\epsilon^k)\exp(-\tilde{H}_2\epsilon^l) = \exp([\tilde{H}_1, \tilde{H}_2]\epsilon^{k+l}) + \mathcal{O}(\epsilon^{k+l+1}) \tag{20}$$

where the parameter $\epsilon < 1$ will represent the strength of a systematic error.

2. *Euler Decomposition*

In Section III.A.1, it was shown that any one-qubit operation $U \in \mathsf{SU}(2)$ may be written in the form $U = \exp(-\mathrm{i}t\boldsymbol{u}\cdot\boldsymbol{H})$. It is well known that an alternative representation exists, namely the Euler decomposition

$$U = \exp(-\mathrm{i}\alpha_3 H_\mathrm{x})\exp(-\mathrm{i}\alpha_2 H_\mathrm{y})\exp(-\mathrm{i}\alpha_1 H_\mathrm{x}) \tag{21}$$

which is given by sequential rotations by the angles $\{\alpha_1, \alpha_2, \alpha_3\}$ about the H_x, H_y, and H_x axes of the Bloch sphere. The Euler decomposition gives the form of a pulse sequence that produces any arbitrary one-qubit gate. The Euler decomposition also gives a method of producing rotations generated by a Hamiltonian outside of direct control. For example, at perfect resonance $U = \exp(-\mathrm{i}\theta H_z)$ cannot be directly produced; however, the Euler decomposition for the same operation $U = \exp(-\mathrm{i}\frac{\pi}{2}H_\mathrm{x})\exp(-\mathrm{i}\theta H_\mathrm{y})\exp(\mathrm{i}\frac{\pi}{2}H_\mathrm{x})$ may be implemented.

3. *Cartan Decomposition*

Let $\mathfrak{g}$ be a semi-simple Lie algebra that may be decomposed into two subspaces $\mathfrak{g} = \mathfrak{k} \oplus \mathfrak{m}$, $\mathfrak{m} = \mathfrak{k}^\perp$ satisfying the commutation relations

$$[\mathfrak{k}, \mathfrak{k}] \subseteq \mathfrak{k}, \qquad [\mathfrak{m}, \mathfrak{k}] \subseteq \mathfrak{m}, \qquad [\mathfrak{m}, \mathfrak{m}] \subseteq \mathfrak{k} \tag{22}$$

Such a decomposition is called a Cartan decomposition of $\mathfrak{g}$ [10]. Suppose for the moment a subalgebra $\mathfrak{a}$ of $\mathfrak{g}$ is in a subspace of $\mathfrak{m}$. Because $\mathfrak{a}$ is an algebra of its own right, it is closed under the Lie bracket $[\mathfrak{a}, \mathfrak{a}] \subseteq \mathfrak{a}$. However, note $\mathfrak{a} \subseteq \mathfrak{m}$ implies that $[\mathfrak{a}, \mathfrak{a}] \subseteq [\mathfrak{m}, \mathfrak{m}] \subseteq \mathfrak{k}$. Because the subspaces $\mathfrak{k}$ and $\mathfrak{m}$ are mutually

orthogonal, then $[\mathfrak{a}, \mathfrak{a}] = \{0\}$ and the subalgebra $\mathfrak{a}$ must be abelian. A maximal abelian subalgebra $\mathfrak{a} \subseteq \mathfrak{m}$ for a Cartan decomposition pair $(\mathfrak{k}, \mathfrak{m})$ is called a Cartan subalgebra [10].

For brevity, we state without proof an important theorem regarding the decomposition of an operator in a group G with a Lie algebra admitting a Cartan decomposition. Consider a Lie algebra $\mathfrak{g}$ with a Cartan subalgebra $\mathfrak{a}$ corresponding to the decomposition pair $(\mathfrak{k}, \mathfrak{m})$. Every U in the group $\mathsf{G} = \mathrm{e}^{\mathfrak{g}}$ may be written in the form

$$U = K_2 A K_1 \tag{23}$$

where $K_1, K_2 \in \mathrm{e}^{\mathfrak{k}}$, and $A \in \mathrm{e}^{\mathfrak{a}}$. This is called the KAK Cartan decomposition for the group G. The interested reader is referred to Ref. [35] for additional details regarding the KAK decomposition.

As a relevant example, here we show how the Euler decomposition for a propagator $U \in \mathsf{SU}(2)$ is a special case of a KAK decomposition. The algebra is spanned by the orthogonal basis matrices $\mathfrak{su}(2) = \mathrm{span}\{-\mathrm{i}H_\mathrm{x}, -\mathrm{i}H_\mathrm{y}, -\mathrm{i}H_\mathrm{z}\}$. Observe that $\mathfrak{k} = \mathrm{span}\{-\mathrm{i}H_\mathrm{x}\}$ and $\mathfrak{m} = \mathrm{span}\{-\mathrm{i}H_\mathrm{y}, -\mathrm{i}H_\mathrm{z}\}$ form a Cartan decomposition for $\mathfrak{su}(2)$. The maximal abelian subalgebra of $\mathfrak{m}$ is one-dimensional; we choose $\mathfrak{a} = \mathrm{span}\{-\mathrm{i}H_\mathrm{y}\}$ although the choice $\mathfrak{a}' = \mathrm{span}\{-\mathrm{i}H_\mathrm{z}\}$ would serve just as well (i.e., the different axis conventions of the Euler decomposition differ in the choice of a maximal abelian subalgebra). Then by Eq. (23), every element $U \in \mathsf{SU}(2)$ may be expressed in the form $U = \exp(-\mathrm{i}\alpha_3 H_\mathrm{x}) \exp(-\mathrm{i}\alpha_2 H_\mathrm{y}) \exp(-\mathrm{i}\alpha_1 H_\mathrm{x})$, where the parameters α_j are real. This restatement of Eq. (21) completes the proof. The KAK decomposition is an existence theorem, and does not provide a direct method for the calculation of the required rotation angles α_j.

The Cartan decomposition has important implications for universality. For instance, if one may generate any unitary operation over the subgroups $\mathrm{e}^{\mathfrak{k}}$ and $\mathrm{e}^{\mathfrak{a}}$, then any gate in the larger group $\mathrm{e}^{\mathfrak{g}}$ may be produced. Similarly, if compensation sequences exist for operations in these subgroups, then they may be combined in the KAK form to yield a compensating pulse sequence for an operation in the larger group. Another important application is the decomposition of large Lie groups into products of more simple ones. Of special interest to quantum computing is the inductive decomposition of n-qubit $\mathsf{SU}(2^n)$ gates into products of one-qubit $\mathsf{SU}(2)$ and two-qubit $\mathsf{SU}(4)$ rotations [50].

IV. COMPOSITE PULSE SEQUENCES ON SU(2)

In this section, we study pulse sequences that compensate single-qubit operations, which form a representation of the group $\mathsf{SU}(2)$. Our approach is to use Lie

theoretic methods to study the effects of composite rotations. Topologically, sequences of infinitesimal rotations may be interpreted as paths in the neighborhood of the group identity. It is frequently easier to construct sequences of infinitesimal paths on the Lie algebra, and then map these sequences to the manifold of group operations. Several techniques will be used to construct compensating pulse sequences of arbitrary accuracy, including techniques that use Solovay–Kitaev methods and Trotter formulas.

A. Solovay–Kitaev Sequences

The Solovay–Kitaev sequences, so named because the construction of the higher-order sequences involves the identity Eq. (20) used by Kitaev in his proof of universal control from finite gate sets [49], are among the simplest families of fully compensating composite pulse sequences. The SK sequences were first introduced by Brown et al. [51], and are designed to compensate pulse length, amplitude, and addressing errors using resonant pulses. Here, we show that the SK family of sequences may be derived using the method outlined in Section III.B.1.

1. Narrowband Behavior

Narrowband composite pulse sequences apply a spin rotation over only a narrow range of strengths of the control field [52]. Therefore, they are most suited for correcting addressing errors [34] (i.e., situations where the spatial variation in the field strength is used to discriminate between spins in an ensemble). The operations on the addressed qubits are assumed to be error-free, whereas on the unaddressed qubits the imperfect pulses take the form $V(\boldsymbol{u}(t)) = U(\epsilon_N \boldsymbol{u}(t))$, where $\epsilon_N < 1$ is the systematic addressing error amplitude (see Section II.B.1). Narrowband sequences are a means of applying a target operation U_T on the addressed spins while removing the leading effects of the operation on the unaddressed spins. For a composite pulse sequence to exhibit nth-order narrowband behavior, we require that two conditions must be satisfied: first that for the unaddressed qubits the sequence $V(\boldsymbol{u}(t))$ approximates the identity up to $\mathcal{O}(\epsilon_N^{n+1})$, and second, that on the targeted spins the desired operation is applied without error.

From a mathematical perspective, systematic addressing errors are among the easiest to consider. Note that for the unaddressed qubits the ideal values for the controls $\boldsymbol{u}(t)$ is zero (ideally no operation takes place). This implies $H_\mu^I(t) = H_\mu$, and that the Schrödinger and interaction frames in Eq. (8) are identical. We may develop a sequence that corrects the control distortion without the added complication of the passage into an interaction picture. For this reason, we first study narrowband sequences before considering other error models.

Sequences with first-order narrowband properties may be constructed using the method described in Section III.B.1. We consider sequences composed of three

square pulses (i.e., piecewise constant control functions), which produce the ideal propagation:

$$U(\boldsymbol{u}(t)) = \prod_{k=1}^{3} U_k, \qquad U_k = \exp(-\mathrm{i}t_k \boldsymbol{u}_k \cdot \boldsymbol{H}) \tag{24}$$

On an addressed qubit, $U(\boldsymbol{u}(t))$ is implemented, whereas on the unaddressed qubits $V(\boldsymbol{u}(t)) = U(\epsilon_N \boldsymbol{u}(t))$ is applied. We may use either a BCH or Magnus expansion to compute the applied operation on the unaddressed qubit. From Eq. (17) and the error model $v_{\mathrm{x/y}}(t) = \epsilon_N u_{\mathrm{x/y}}(t)$, the first-order term is

$$\epsilon_N \Omega_1 = -\mathrm{i}\epsilon_N (t_3 \boldsymbol{u}_3 + t_2 \boldsymbol{u}_2 + t_1 \boldsymbol{u}_1) \cdot \boldsymbol{H} \tag{25}$$

The spin operators $-\mathrm{i}H_\mu \in \{-\mathrm{i}H_\mathrm{x}, -\mathrm{i}H_\mathrm{y}, -\mathrm{i}H_\mathrm{z}\}$ form an orthogonal basis for $\mathfrak{su}(2)$, and the terms $-\mathrm{i}\epsilon_N t_k \boldsymbol{u}_k \cdot \boldsymbol{H}$ may be regarded as vectors on the dynamical Lie algebra. In order to eliminate the first-order Magnus term $\epsilon_N \Omega_1$, the sum of the components must equal zero, that is, the vectors must form a closed triangular path. Such paths may be found using elementary geometric methods.

It is important at this point to allow experimental considerations to place constraints on the sequences under study. For instance, in many cases it is desirable to perform coherent operations at resonance, a condition that forces the vectors to lie in the H_x–H_y plane. One possible choice is

$$\begin{aligned}
-\mathrm{i}\epsilon_N t_1 \boldsymbol{u}_1 \cdot \boldsymbol{H} &= -\mathrm{i}\epsilon_N \theta H_\mathrm{x} \\
-\mathrm{i}\epsilon_N t_2 \boldsymbol{u}_2 \cdot \boldsymbol{H} &= -\mathrm{i}\epsilon_N 2\pi(\cos\phi_{\mathrm{SK1}} H_\mathrm{x} + \sin\phi_{\mathrm{SK1}} H_\mathrm{y}) \\
-\mathrm{i}\epsilon_N t_3 \boldsymbol{u}_3 \cdot \boldsymbol{H} &= -\mathrm{i}\epsilon_N 2\pi(\cos\phi_{\mathrm{SK1}} H_\mathrm{x} - \sin\phi_{\mathrm{SK1}} H_\mathrm{y})
\end{aligned} \tag{26}$$

where the phase $\phi_{\mathrm{SK1}} = \arccos(-\theta/4\pi)$ is selected so that $\epsilon_N \sum_k t_k \boldsymbol{u}_k = 0$, and therefore the first-order expansion term $\epsilon_N \Omega_1 = 0$ is eliminated. Figure 5a is a diagram of these vectors on $\mathfrak{su}(2)$, where the sequence may be represented as a closed isosceles triangle with one segment aligned on the $-\mathrm{i}H_\mathrm{x}$ axis.

For clarity, we use the notation $R(\theta, \phi) = \exp(-\mathrm{i}\theta(\cos\phi H_\mathrm{x} + \sin\phi H_\mathrm{y}))$ to represent propagators that induce rotations about an axis in the H_x–H_y plane. Observe that for resonant square-pulse operations in $\mathsf{SU}(2)$, $R(\theta, \phi) = U(\boldsymbol{u}_k; t_k, 0)$, where $\boldsymbol{u}_k = \Omega(\cos\phi, \sin\phi, 0)$ and $\theta = t_k|\boldsymbol{u}_k|$. We also define the corresponding imperfect propagator $M(\theta, \phi) = V(\boldsymbol{u}; t_k, 0)$, and recall that the imperfect propagators on the unaddressed qubits $M(\theta, \phi) = R(\theta\epsilon_N, \phi)$ and addressed qubits $M(\theta, \phi) = R(\theta, \phi)$ have different implied dependencies on the systematic error. Then combining Eqs. (24) and (26), the propagator may be written as

$$\begin{aligned}
U(\epsilon_N \boldsymbol{u}(t)) &= R(2\pi\epsilon_N, -\phi_{\mathrm{SK1}}) R(2\pi\epsilon_N, \phi_{\mathrm{SK1}}) R(\theta\epsilon_N, 0) = \mathbb{1} + \mathcal{O}(\epsilon_N^2) \\
M_{\mathrm{SK1}}(\theta, 0) &= M(2\pi, -\phi_{\mathrm{SK1}}) M(2\pi, \phi_{\mathrm{SK1}}) M(\theta, 0)
\end{aligned} \tag{27}$$

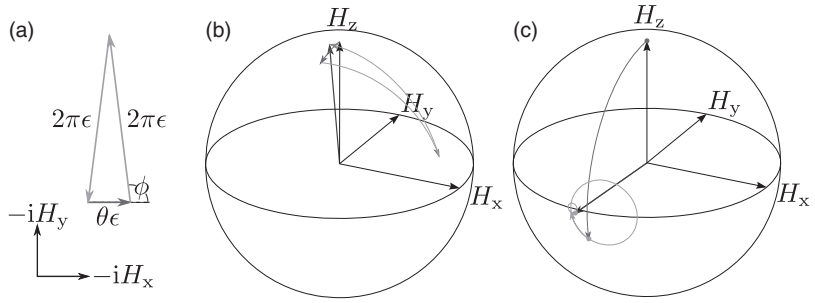

Figure 5. (**a**) Vector path followed by SK1 on the Lie algebra. (**b**) Trajectory of an unaddressed spin during an SK1 sequence, using imperfect rotations of the form $M(\theta, \phi) = R(\theta\epsilon_N, \phi)$. (**c**) SK1 correcting an amplitude error, using imperfect $M(\theta, \phi) = R(\theta(1 + \epsilon_A), \phi)$. In these plots $\epsilon_N = \epsilon_A = 0.2$.

for the unaddressed qubits, and as

$$\begin{aligned} U(\boldsymbol{u}(t)) &= R(2\pi, -\phi_{\mathrm{SK1}})R(2\pi, \phi_{\mathrm{SK1}})R(\theta, 0) \\ M_{\mathrm{SK1}}(\theta, 0) &= M(2\pi, -\phi_{\mathrm{SK1}})M(2\pi, \phi_{\mathrm{SK1}})M(\theta, 0) \end{aligned} \tag{28}$$

for addressed qubits. This is the first-order Solovay–Kitaev sequence, here denoted as SK1. On the addressed qubits the rotations $R(2\pi, \phi_{\mathrm{SK1}}) = R(2\pi, -\phi_{\mathrm{SK1}}) = -\mathbb{1}$ are resolutions of the identity and the effect of the sequence is to apply the target unitary $U_T = R(\theta, 0)$, whereas on the unaddressed spins the sequence applies $\mathbb{1} + \mathcal{O}(\epsilon_N^2)$ and the leading first-order rotation of the unaddressed spins is eliminated. Therefore, SK1 satisfies the conditions for narrowband behavior. When the sequence SK1 is used in the place of the simple rotation $R(\theta, 0)$, the discrimination between addressed and unaddressed spins is enhanced.

2. *Broadband Behavior*

Broadband composite pulses apply a spin rotation over a large range of strengths of the control field and are best suited for correcting systematic amplitude and pulse-length errors that correspond to systematic over- and underrotations during qubit manipulations. Broadband sequences are a means of applying a target operation in the presence of inaccurate field strengths or pulse durations. When we require for a sequence to exhibit nth-order broadband behavior, the effect of the sequence is to approximate the target operation U_T up to $\mathcal{O}(\epsilon_A^n)$ in the case of amplitude errors, or up to $\mathcal{O}(\epsilon_T^n)$ in the case of pulse-length errors. As before, it is convenient to consider sequences comprised of resonant square pulses. In this case the amplitude and pulse length error models are in some sense equivalent because they both apply a proportional distortion to the $u_x(t)$ and $u_y(t)$ controls. In the following discussion

we will explicitly use the amplitude error model, where imperfect rotations take the form $M(\theta, \phi) = R(\theta(1 + \epsilon_A), \phi)$.

We now show how a Solovay–Kitaev sequence with first-order broadband properties may be derived. Although the method presented in Section III.A.1 may be applied, here a more direct technique is used. Our strategy is to construct a pulse sequence entirely out of imperfect rotations $M(\theta, \phi) = R(\theta(1 + \epsilon_A), \phi) = R(\theta\epsilon_A, \phi)R(\theta, \phi)$ using Eq. (27) as a template. Explicitly, this is achieved with the matrix manipulations

$$\begin{aligned} R(\theta, 0) + \mathcal{O}(\epsilon_A^2) &= R(2\pi\epsilon_A, -\phi_{\mathrm{SK1}})R(2\pi\epsilon_A, \phi_{\mathrm{SK1}})R(\theta\epsilon_A, 0)R(\theta, 0) \\ &= R(2\pi\epsilon_A, -\phi_{\mathrm{SK1}})R(2\pi, -\phi_{\mathrm{SK1}})R(2\pi\epsilon_A, \phi_{\mathrm{SK1}}) \\ &\quad \times R(2\pi, \phi_{\mathrm{SK1}})R(\theta\epsilon_A, 0)R(\theta, 0) \end{aligned}$$

where we have right-multiplied Eq. (27) by $R(\theta, 0)$ (after substituting ϵ_A for ϵ_N) and inserted the identity $R(2\pi, \phi_{\mathrm{SK1}}) = R(2\pi, -\phi_{\mathrm{SK1}}) = -\mathbb{1}$. Then, by combining rotations about the same axis, one obtains the result,

$$\begin{aligned} U((1 + \epsilon_A)\boldsymbol{u}(t)) &= R(2\pi(1 + \epsilon_A), -\phi_{\mathrm{SK1}})R(2\pi(1 + \epsilon_A), \phi_{\mathrm{SK1}})R(\theta(1 + \epsilon_A), 0) \\ M_{\mathrm{SK1}}(\theta, 0) &= M(2\pi, -\phi_{\mathrm{SK1}})M(2\pi, \phi_{\mathrm{SK1}})M(\theta, 0) = R(\theta, 0) + \mathcal{O}(\epsilon_A^2) \quad (29) \end{aligned}$$

where again $\phi_{\mathrm{SK1}} = \arccos(-\theta/4\pi)$. In the presence of unknown amplitude errors, the sequence reduces the effect of the error while applying the effective rotation $R(\theta, 0)$. Observe that in terms of imperfect rotations this is the same SK1 sequence derived earlier. SK1 has both narrowband and broadband behavior, and the sequence may correct both addressing and amplitude errors simultaneously. Such a sequence is called a *passband* sequence.

3. *Generalization to Arbitrary Gates in* SU(2)

The sequence SK1 is designed to compensate single-qubit rotations about the H_x axis. If this sequence is to be useful in quantum computation, it must be generalized so that any single-qubit rotation may be corrected. One method involves transforming the sequence by a similarity transformation of the pulse propagators. As an example, suppose we require an SK1 sequence that performs the rotation $R(\theta, \phi) = \exp(-\mathrm{i}\phi H_z)R(\theta, 0)\exp(\mathrm{i}\phi H_z)$ on the addressed spins. Similarity transformation of pulses under $\exp(-\mathrm{i}\phi H_z)$ represent a phase advance in the rotating frame. It is evident that the transformed sequence

$$M_{\mathrm{SK1}}(\theta, \phi) = M(2\pi, \phi - \phi_{\mathrm{SK1}})M(2\pi, \phi + \phi_{\mathrm{SK1}})M(\theta, \phi) \quad (30)$$

performs the desired compensated rotation. In this manner, a compensating pulse sequence for any target operation $U_T \in \mathrm{SU}(2)$ may be constructed. One may solve for the operation Υ that performs the planar rotation $\Upsilon U_T \Upsilon^\dagger = R(\theta, 0)$, where

$\theta = ||\log U_T||_{\mathrm{HS}}/||H_{\mathrm{x}}||_{\mathrm{HS}}$. Then the transformed sequence $\Upsilon^{\dagger} M_{\mathrm{SK1}}(\theta, 0)\Upsilon$ performs a first-order compensated U_T operation. Similarity transformations of pulse sequence propagators can be extremely useful and are frequently applied in composite pulse sequences.

Alternative methods exist for generating an arbitrary compensated rotations. Recall from Section III.C.2 that any operation $U_T \in \mathsf{SU}(2)$ may be expressed in terms of a Euler decomposition $U_T = R(\alpha_3, 0)R(\alpha_2, \pi/2)R(\alpha_1, 0)$. An experimentalist may apply U_T by implementing each of the Euler rotations in sequence, however, in the presence of an unknown systematic error each of the applied rotations is imperfect and the fidelity of the applied gate is reduced. The error may be compensated by replacing each imperfect pulse with a compensating pulse sequence. For example, the sequence

$$M_{\mathrm{SK1}}(\alpha_3, 0)M_{\mathrm{SK1}}(\alpha_2, \pi/2)M_{\mathrm{SK1}}(\alpha_1, 0) = U_T + \mathcal{O}(\epsilon_A^2) \tag{31}$$

compensates amplitude errors to first-order by implementing SK1 sequences for each of the rotations in an Euler decomposition for U_T. This construction is an example of pulse sequence concatenation. By concatenating two independent pulse sequences, it is sometimes possible to produce a sequence with properties inherited from each parent sequence.

4. Arbitrarily Accurate SK Sequences

In this section, we discuss the Solovay–Kitaev method for constructing arbitrarily accurate composite pulse sequences, which may be used to systematically improve the performance of an initial seed sequence. The Lie algebraic picture is particularly helpful in the description of the algorithm. The method is quite general, and can be used on sequences other than SK1.

Suppose that we have an nth-order compensating pulse sequence, here denoted as W_n. The problem we consider is the identification of a unitary operator A_{n+1} such that $W_{n+1} = A_{n+1}W_n = U_T + \mathcal{O}(\epsilon^{n+2})$, where W_{n+1} is an $(n+1)$th-order sequence. Assume for now that such an operator exists, and consider that in the presence of systematic errors, the application of the correction gate A_{n+1} is imperfect. However, if it is possible to implement a compensating pulse sequence B_{n+1}, which is an $\mathcal{O}(\epsilon^{n+2})$ approximation of A_{n+1}, then it is still possible to construct an $(n+1)$th-order sequence

$$W_{n+1} = B_{n+1}W_n = U_T + \mathcal{O}(\epsilon^{n+2}) \tag{32}$$

We may then continue constructing pulse sequences of increasing accuracy in this fashion if there exists a family of operators $\{A_{n+1}, A_{n+2}, A_{n+3}, \cdots A_m\}$ and a corresponding family of pulse sequences $\{B_{n+1}, B_{n+2}, B_{n+3}, \cdots B_m\}$ that

implement the operators to the required accuracy. This immediately suggests an inductive construction for the sequence W_m

$$W_m = B_m\, B_{m-1} \cdots B_{n+3}\, B_{n+2}\, B_{n+1}\, W_n = U_T + \mathcal{O}(\epsilon^{m+1}) \tag{33}$$

This is the basis of the Solovay–Kitaev method [51]. To apply the method, we must first have a means of calculating the correction A_{n+1}, and second we must find a compensating sequence B_{n+1} robust to the systematic error model considered.

We turn our attention to the calculation of the correction terms A_{n+1}. It is convenient to decompose the pulse sequence propagator using an interaction frame as $W_n = U_T U^I(\epsilon \boldsymbol{\delta u}(t))$, where $U_T = U(\boldsymbol{u}(t))$ is the target gate. In the spirit of Eq. (16), a Magnus expansion for $U^I(\epsilon \boldsymbol{\delta u}(t))$ may be used. Observe that $W_n = U_T \exp(\epsilon^{n+1}\Omega_{n+1}) + \mathcal{O}(\epsilon^{n+2})$. Then letting $A_{n+1} = U_T \exp(-\epsilon^{n+1}\Omega_{n+1}) U_T^\dagger$ it may be verified using the BCH formula that $A_{n+1} W_n = U_T + \mathcal{O}(\epsilon^{n+2})$. This result may also be interpreted in terms of vector displacements on the Lie algebra. In the interaction frame, $\epsilon^{n+1}\Omega_{n+1}$ may be interpreted as a vector in $\mathfrak{su}(2)$. Similarly, the infinitesimal rotation A_{n+1} corresponds to the vector $-\epsilon^{n+1}\Omega_{n+1}$, equal in magnitude and opposite in orientation. The first-order term of the BCH series corresponds to vector addition on the Lie algebra, and the $\mathcal{O}(\epsilon^{n+1})$ terms cancel.

What remains is to develop a compensating pulse sequence that implements A_{n+1} to the required accuracy under a given error model. Let us define $P_{jz}(\alpha) = \exp(-\mathrm{i}\alpha\epsilon^j H_z) + \mathcal{O}(\epsilon^{j+1})$ and also the rotated analogues $P_{jx}(\alpha) = \exp(-\mathrm{i}\alpha\epsilon^j H_x) + \mathcal{O}(\epsilon^{j+1})$ and $P_{jy}(\alpha) = \exp(-\mathrm{i}\alpha\epsilon^j H_y) + \mathcal{O}(\epsilon^{j+1})$. Frequently if one such P_j may be produced, then often the remaining two may be produced by similarity transformation of the propagators or by using an Euler decomposition. At this point we use Eq. (20), used in the proof for the Solovay–Kitaev theorem, to construct relation

$$P_{kx}(-\alpha) P_{\ell y}(-\beta) P_{kx}(\alpha) P_{\ell y}(\beta) = P_{jz}(\alpha\beta), \qquad k + \ell = j \tag{34}$$

Continuing in this manner, each of the P_js may be recursively decomposed into a product of first-order propagators $P_{1k}(\alpha) = \exp(-\mathrm{i}\alpha\epsilon H_k) + \mathcal{O}(\epsilon^2)$. Our strategy is to use Eq. (34) to implement $P_{(n+1)z}(\xi)$ where $\xi = ||\Omega_{n+1}||_{\mathrm{HS}}/||H_z||_{\mathrm{HS}}$. On the Lie algebra, this operation is represented by vector of length $\epsilon^{n+1}||\Omega_{n+1}||_{\mathrm{HS}}$ oriented along the $-\mathrm{i}H_z$ axis. Let Υ be the rotation that performs $\Upsilon\Omega_{n+1}\Upsilon^\dagger = \mathrm{i}\xi H_z$ (i.e., the operator that rotates Ω_{n+1} onto the $\mathrm{i}H_z$ axis). Then, by similarity transformation under $U_T\Upsilon^\dagger$

$$U_T\Upsilon^\dagger P_{(n+1)z}(\xi)\Upsilon U_T^\dagger = U_T \exp(-\epsilon^{n+1}\Omega_{n+1}) U_T^\dagger + \mathcal{O}(\epsilon^{n+2}) = B_{n+1} \tag{35}$$

the sequence $P_{(n+1)z}(\xi)$ may be transformed into precisely the required correction sequence needed for the Solovay–Kitaev method. There are two approaches for applying the transformation by $U_T\Upsilon^\dagger$: we may either calculate the transformed analogues of each of the pulses in $P_{(n+1)z}(\xi)$ and then apply the transformed pulses,

or we may, when possible, directly include the transformation pulses (or an estimate for them) as physically applied pulses in the sequence. The second approach is only viable when it is possible to generate accurate inverse operations $\Upsilon U_T^\dagger$ [53].

Our construction will be complete once we have a method for generating the simple "pure-error" propagator $P_{1x}(\alpha)$. In many cases it is sufficient to only consider $P_{1x}(\alpha)$ because the other propagators $P_{1y}(\alpha)$ and $P_{1z}(\alpha)$ are related by a similarity transformation. In general, the method will depend on the error model under consideration; here we explicitly show how to construct this term in the amplitude and pulse-length error models and also in the addressing error model.

a. Addressing Errors. We wish to perform the evolution $P_{1x}(\alpha)$ using a product of imperfect square-pulse propagators $M(\theta, \phi)$. Recall that in this model rotations on the addressed qubit are error free $M(\theta, \phi) = R(\theta, \phi)$, whereas on the unaddressed qubit the applied unitary depends on the systematic addressing error $M(\theta, \phi) = R(\theta\epsilon_N, \phi)$. Similarly, the sequence implementing $P_{1x}(\alpha)$ must resolve to the identity on the addressed qubit, while on the unaddressed qubit $\exp(-\mathrm{i}\alpha\epsilon_N H_x) + \mathcal{O}(\epsilon_N^2)$ is applied. This behavior may be achieved by using a pulse sequence to implement P_{1x}. Let

$$S_x(\alpha) = M(2\pi a, -\phi_\alpha)M(2\pi a, \phi_\alpha) \tag{36}$$

where $a = \lceil |\alpha|/4\pi \rceil$ is a integer number of 2π rotations and $\phi_\alpha = \arccos(\alpha/4\pi a)$. On the addressed qubit, $S_x(\alpha)$ resolves to the identity, whereas for the unaddressed spins,

$$S_x(\alpha) = M(2\pi a, -\phi_\alpha)M(2\pi a, \phi_\alpha) = R(2\pi a\epsilon_N, -\phi_\alpha)R(2\pi a\epsilon_N, \phi_\alpha) = P_{1x}(\alpha)$$

is applied. In the Lie algebraic picture, $S_x(\alpha)$ is composed of two vectors constructed so that their vector sum is $-\mathrm{i}\alpha\epsilon_N H_x$. Similarly, $S_y(\beta) = M(2\pi b, \pi/2 - \phi_\beta)M(2\pi b, \pi/2 + \phi_\beta) = P_{1y}(\beta)$. From these basic sequences, we may construct $P_{2z}(\alpha\beta)$ by using the balanced group commutator Eq. (34). In Fig. 6a, we plot the

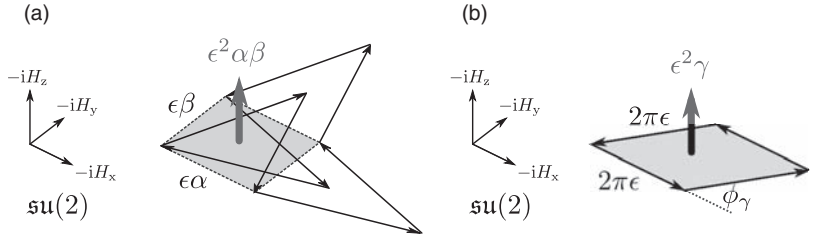

Figure 6. Generation of the pure error term in the Solovay–Kitaev method. (**a**) From Eq. (34), $P_{2z}(\alpha\beta)$ may be produced by the sequence $S_x(-\alpha)S_y(-\beta)S_x(\alpha)S_y(\beta)$. On the Lie algebra the sequence corresponds to a closed rectangular path with an enclosed area of $\epsilon^2\alpha\beta$. (**b**) Alternatively, the rhombus construction may be used to generate $P_{2z}(\alpha)$ using four pulses.

sequence $P_{2z}(\alpha\beta)$ as a vector path on the Lie algebra. The sequence encloses a signed area $\epsilon_N^2\alpha\beta$, which is denoted by the shaded rectangular figure. By tuning the rotation angles α and β, one may generate a term that encloses any desired area, thus allowing the synthesis of an arbitrary pure-error term.

At this point, we discuss a subtle feature of the addressing error model, which at first appears to complicate the application of the SK method. Observe that on the unaddressed spin, the imperfect propagators may only apply small rotations (i.e., rotations by angles $\theta\epsilon_N$). If we restrict ourselves to sequences composed of resonant square pulses, then the term proportional to $P_{1z}(\alpha)$ may not be produced; we may not prepare such a term by similarity transformation (e.g., $R(\pi/2, 0)S_y(\alpha)R^\dagger(\pi/2, 0)$) because such an operation would either require a large rotation or if instead the transformation was carried out on the individual sequence propagators, the rotation axes would be lifted out of the H_x–H_y plane. Similar arguments show that the Euler decomposition is also unavailable.

Fortunately, this restriction is not as serious as it first appears; the SK method may be used provided that the sequence terms are chosen with care. We are ultimately saved by the orientation of the error terms in the Lie algebra. Using the BCH formula, it is straightforward to show that for sequences composed of resonant pulses, the even-order error terms are always aligned along the $-\mathrm{i}H_z$ axis, whereas the odd-order terms are confined to $H_x - H_y$ plane. Likewise, using only $S_x(\alpha)$ and $S_y(\beta)$, it is possible to generate correction terms that follow the same pattern. As a consequence, in this case it is possible to generate the correction terms $U_T \exp(-\epsilon_N^{n+1}\Omega_{n+1})U_T^\dagger$ by carefully choosing the rotation angles and phases in the correction sequence B_{n+1}.

As an instructive example, we shall derive a second-order passband sequence using the Solovay–Kitaev method. We begin by calculating the Magnus expansion for the seed sequence $M_{\mathrm{SK1}}(\theta, 0) = U_T \exp(\epsilon_N^2\Omega_2 + \epsilon_N^3\Omega_3 + \cdots)$ where the target operation $U_T = \mathbb{1}$ for the unaddressed qubit. To cancel the second-order term, we simply need to apply the inverse of $\exp(\epsilon_N^2\Omega_2) = \exp(-\mathrm{i}2\pi^2\epsilon_N^2 \sin(2\phi_{\mathrm{SK1}})H_z)$. The planar rotation $\Upsilon = \mathbb{1}$, since $B_2 = P_{2z}(-2\pi^2 \sin(2\phi_{\mathrm{SK1}}))$ is already oriented in the correct direction. One possible choice for B_2 is the sequence

$$B_2 = S_x(-2\pi\cos\phi_{\mathrm{SK1}})S_y(2\pi\sin\phi_{\mathrm{SK1}})S_x(2\pi\cos\phi_{\mathrm{SK1}})S_y(-2\pi\sin\phi_{\mathrm{SK1}}) \quad (37)$$

The sequence $M_{\mathrm{SK2}}(\theta, 0) = B_2 M_{\mathrm{SK1}}(\theta, 0) = U_T + \mathcal{O}(\epsilon_N^3)$ corrects addressing errors to second order. We denote an nth order compensating sequence produced by the Solovay–Kitaev method using SK1 as an initial seed as SKn; here we have produced an SK2 sequence.

More efficient constructions for the correction sequence B_2 exist. Observe that we may directly create the pure error term $P_{2z}(\gamma)$ by using four pulses in the balanced group commutator arrangement $P_{2z}(\gamma) = M^\dagger(2\pi c, \phi_\gamma)M^\dagger(2\pi c, \phi'_\gamma)$ $M(2\pi c, \phi_\gamma)M(2\pi c, \phi'_\gamma)$, where $c = \lceil|\gamma|/4\pi\rceil$ and the phases are chosen to be $\phi_\gamma = \arcsin(\gamma/4\pi^2c^2)$ and $\phi'_\gamma = (1 - \mathrm{sign}\gamma)\pi/2$. The phase ϕ'_γ is only necessary to

ensure that the construction also works for negative γ. We call this arrangement the rhombus construction. In Fig. 6b, we plot this sequence as a vector path on $\mathfrak{su}(2)$. In this construction the magnitude of the error term is tuned by adjusting the phase ϕ_γ (i.e., adjusting the area enclosed by the rhomboidal path of the sequence in the Lie algebra). The rhombus construction has the advantage of requiring half as many pulses as the standard method. We will now use this construction to produce an alternative form for SK2. Let

$$B_2' = M(2\pi, \phi_\gamma + \pi)M(2\pi, 0)M(2\pi, \phi_\gamma)M(2\pi, \pi) \tag{38}$$

where $\phi_\gamma = \arcsin(\sin(2\phi_{\mathrm{SK1}})/2)$. Then $M'_{\mathrm{SK2}}(\theta, 0) = B_2' M_{\mathrm{SK1}}(\theta, 0) = U_T + \mathcal{O}(\epsilon_N^3)$.

b. Amplitude/Pulse-Length Errors. We now turn our attention to the compensation of amplitude and pulse-length errors. When considering these error models, the imperfect propagators of the form $M(\theta, \phi) = R(\theta(1 + \epsilon_A), \phi)$. In this case, we may also construct P_{1x} using Eq. (36) since the imperfect 2π rotations reduce to $M(2\pi a, \phi) = R(2\pi a \epsilon_A, \phi)$ and $S_x(\alpha) = P_{1x}(\alpha)$. As a consequence, if the initial seed sequence W_n is a passband sequence then W_{n+1} is also a passband sequence. We note however, that in this error model, one has more flexibility in the synthesis of the correction sequences B_{n+1} because now the imperfect propagators apply large rotations, then we may perform similarity transformations of sequences by directly implementing the required pulses. Notably, we may use imperfect propagators of order $\mathcal{O}(\epsilon_A^n)$ to apply a desired transformation at a cost of an error of order $\mathcal{O}(\epsilon_A^{n+1})$, for example, $M(\theta, \phi)P_{jz}M^\dagger(\theta, \phi) = R(\theta, \phi)P_{jz}R^\dagger(\theta, \phi) + \mathcal{O}(\epsilon_A^2)$.

The SK method may be used to calculate higher-order compensation sequences for the amplitude error model. We begin by calculating the relevant Magnus expansion for the seed sequence $M_{\mathrm{SK1}}(\theta, 0) = M(2\pi, -\phi_{\mathrm{SK1}})M(2\pi, \phi_{\mathrm{SK1}})M(\theta, 0) = U_T \exp(\epsilon_A^2 \Omega_2 + \epsilon_A^3 \Omega_3 + \cdots)$ where now in the amplitude error model the target operation $U_T = R(\theta, 0)$. To cancel the second-order term we must apply the inverse of $U_T \exp(\epsilon_A^2 \Omega_2) U_T^\dagger = \exp(-\mathrm{i}2\pi^2 \epsilon_A^2 \sin(2\phi_{\mathrm{SK1}}) H_z)$. This is precisely the same term that arose previously for addressing errors and the error may be compensated the same way. In fact every nth-order SK sequence is passband and works for both error models.

B. Wimperis/Trotter-Suzuki Sequences

In this section, we study a second family of fully compensating pulse sequences, first discovered and applied by Wimperis [52], which may be used to correct pulse length, amplitude, and addressing errors to second order. These sequences have been remarkably successful and have found extensive use in NMR and quantum information [54–56]. Furthermore, the Wimperis sequences may be generalized to

a family of arbitrarily high-order sequences by connecting them to Trotter-Suzuki formulas [51]. An analogous composite sequence composed of rotations in SU(4) may be used to correct two-qubit operations [57,58]. We study the two-qubit case in Section V.A.

1. *Narrowband Behavior*

We begin with the problem of identifying narrowband sequences that correct addressing errors. In the addressing error model, operations on addressed qubits are error free, whereas on the unaddressed qubits the imperfect propagators takes the form $V(\boldsymbol{u}(t)) = U(\epsilon_N \boldsymbol{u}(t))$ and $U_T = \mathbb{1}$. Further, we shall constrain ourselves to sequences composed of resonant square-pulse propagators. Specifically, we search for arrangements of four pulses that eliminate both the first- and second-order Magnus expansion term for the imperfect propagator.

Before explicitly describing the construction of the Wimperis sequences, we digress shortly to point out a certain symmetry property that may be used to ensure that $\epsilon_N^2 \Omega_2 = 0$. Consider the group product of propagators of the form,

$$U(\epsilon_N \boldsymbol{u}(t)) = U_2 U_3 U_2 U_1, \qquad U_k = \exp(-\mathrm{i}\epsilon_N t_k \boldsymbol{u}_k \cdot \boldsymbol{H}) \tag{39}$$

with the added condition that the first-order expansion term for $U(\epsilon_N \boldsymbol{u}(t))$ has been already eliminated (i.e. $\epsilon_N \Omega_1 = -\mathrm{i}\epsilon_N (t_3 \boldsymbol{u}_3 + 2t_2 \boldsymbol{u}_2 + t_1 \boldsymbol{u}_1) \cdot \boldsymbol{H} = 0$). In this arrangement, the second and fourth propagators are identical; this pulse symmetry along with $t_1 \boldsymbol{u}_1 + 2t_2 \boldsymbol{u}_2 + t_3 \boldsymbol{u}_3 = 0$ eliminates the second-order term

$$\epsilon_N^2 \Omega_2 = \frac{\epsilon_N^2}{2} \sum_{i=1}^{4} \sum_{j=1}^{i} [-\mathrm{i}t_i \boldsymbol{u}_i \cdot \boldsymbol{H}, -\mathrm{i}t_j \boldsymbol{u}_j \cdot \boldsymbol{H}] = 0 \tag{40}$$

As a consequence, $U(\epsilon_N \boldsymbol{u}(t)) = \mathbb{1} + \mathcal{O}(\epsilon_N^3)$. Alternatively, one may regard the product $T = U_2 U_3 U_2$ as a second-order symmetric Trotter-Suzuki formula for the inverse operation $U_1^\dagger$ [47], which approximately cancels the undesired rotation U_1. Considering the control fields applied during the application of the corrector sequence T, the applied control Hamiltonian is symmetric with respect to time inversion. By a well-known theorem, all even-order expansion terms produced by a time-symmetric Hamiltonian cancel [43,59] (i.e., $\epsilon_N^{2j} \Omega_{2j} = 0$, for all positive integers j). Thus by implementing symmetric corrector sequences T_{2j}, it is sufficient to only consider the cancellation of the remaining odd-order error terms. In Section IV.B.1, we will inductively develop a series of corrector sequences of increasing accuracy based on symmetric Trotter-Suzuki formulas [47,51].

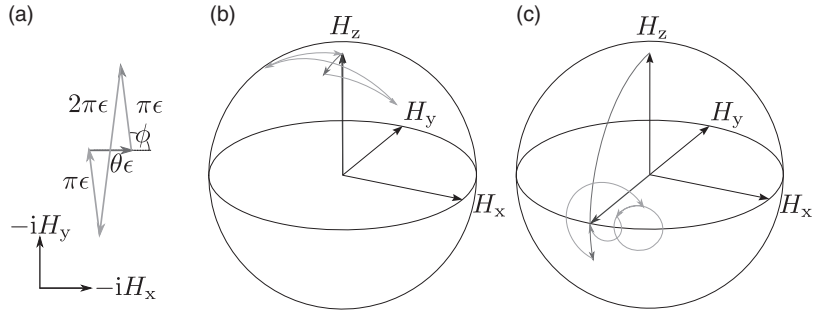

Figure 7. (**a**) Vector path followed by N2 on the Lie algebra. (**b**) Trajectory of an unaddressed spin during an N2 sequence, using imperfect rotations of the form $M(\theta, \phi) = R(\theta\epsilon_A, \phi)$. (**c**) B2 correcting an amplitude error, using imperfect rotations of the form $M(\theta, \phi) = R(\theta(1 + \epsilon_A), \phi)$. In these plots $\epsilon_N = \epsilon_A = 0.2$.

The cancellation of the second-order term may also be inferred from geometric considerations on the Lie algebra. To be concrete, consider a sequence of the form Eq. (39) where

$$\begin{aligned}
\epsilon_N t_1 \boldsymbol{u}_1 \cdot \boldsymbol{H} &= \theta\epsilon_N H_\mathrm{x} \\
\epsilon_N t_2 \boldsymbol{u}_2 \cdot \boldsymbol{H} &= \pi\epsilon_N(\cos\phi_{\mathrm{N2}} H_\mathrm{x} + \sin\phi_{\mathrm{N2}} H_\mathrm{y}) \\
\epsilon_N t_3 \boldsymbol{u}_3 \cdot \boldsymbol{H} &= 2\pi\epsilon_N(\cos\phi_{\mathrm{N2}} H_\mathrm{x} - \sin\phi_{\mathrm{N2}} H_\mathrm{y})
\end{aligned} \tag{41}$$

and the phase is $\phi_{\mathrm{N2}} = \arccos(-\theta/4\pi)$ is chosen so that $t_1\boldsymbol{u}_1 + 2t_2\boldsymbol{u}_2 + t_3\boldsymbol{u}_3 = 0$ (i.e., the vectors form a closed path on the dynamical Lie algebra). Figure 7a is a diagram of these vectors on $\mathfrak{su}(2)$. In $\mathfrak{su}(2)$, the Lie bracket is equivalent to the vector cross-product [35], therefore, we may interpret $||\epsilon_N^2\Omega_2||_{\mathrm{HS}}$ as the signed area enclosed by the vector path on the Lie algebra. We note that the sequence under study encloses two regions of equal area and opposite sign, ensuring that the second-order term is eliminated.

With this insight, the construction of a second-order narrowband sequence is straightforward. The vectors Eq. (41) correspond to the sequence

$$M_{\mathrm{N2}}(\theta, 0) = M(\pi, \phi_{\mathrm{N2}})M(2\pi, -\phi_{\mathrm{N2}})M(\pi, \phi_{\mathrm{N2}})M(\theta, 0) \tag{42}$$

Wimperis refers to this sequence as NB1, which is the established name in the literature. In the current chapter, we label this sequence N2 in anticipation of the generalization of this form to N2j, which compensates addressing errors to $\mathcal{O}(2j)$. We use this language to avoid confusion with other established sequences, namely NB2, NB3, and so on [52]. The N2 sequence may be used to compensate addressing errors. For unaddressed qubits $M(\theta, \phi) = R(\theta\epsilon_N, \phi)$ and thus from Eqs. (40) and (41) it follows that $M_{\mathrm{N2}}(\theta, 0) = \mathbb{1} + \mathcal{O}(\epsilon_N^3)$. Thus, on unaddressed qubits the

sequence performs the identity operation up to second order. Furthermore, for addressed qubits $M(\theta, \phi) = R(\theta, \phi)$ and therefore $M_{\mathrm{N2}}(\theta, 0) = R(\theta, 0)$. As a result, when the sequence $M_{\mathrm{N2}}(\theta, 0)$ is used in the place of the imperfect operation $M(\theta, 0)$, the discrimination between addressed and unaddressed spins is enhanced. In Fig. 7b, we plot the magnetization trajectory for an unaddressed qubit under an N2 sequence.

2. *Broadband Behavior*

As previously discussed, broadband sequences are best suited for correcting amplitude or pulse-length errors. In the following, we will explicitly consider the amplitude error model, where $M(\theta, \phi) = R(\theta(1 + \epsilon_A), \phi) = R(\theta, \phi)R(\theta\epsilon_A, \phi)$. Although a pulse sequence may be studied by considering the interaction frame propagator, the method originally used by Wimperis is simpler. Wimperis's insight was that for lowest orders the toggled frame could be derived geometrically, using the relation $R(\theta, -\phi) = R(\pi, \phi)R(\theta, 3\phi)R(\pi, \phi + \pi)$. Consider the application of the target gate $U_T = R(\theta, 0)$ using the sequence

$$M_{\mathrm{B2}}(\theta, 0) = M(\pi, \phi_{\mathrm{B2}})M(2\pi, 3\phi_{\mathrm{B2}})M(\pi, \phi_{\mathrm{B2}})M(\theta, 0) \tag{43}$$

where $\phi_{\mathrm{B2}} = \arccos(-\theta/4\pi)$. This Wimperis broadband sequence is traditionally called BB1, but here it is denoted as B2. When rewritten in terms of proper rotations one obtains

$$\begin{aligned} M_{\mathrm{B2}}(\theta, 0) &= R(\pi\epsilon_A, \phi_{\mathrm{B2}})\Big(R(\pi, \phi_{\mathrm{B2}})R(2\pi\epsilon_A, \phi_{\mathrm{B2}})R^{\dagger}(\pi, \phi_{\mathrm{B2}})\Big) \\ &\quad \times R(\pi\epsilon_A, \phi_{\mathrm{B2}})R(\theta\epsilon_A, 0)R(\theta, 0) \\ &= \Big[R(\pi\epsilon_A, \phi_{\mathrm{B2}})R(2\pi\epsilon_A, -\phi_{\mathrm{B2}})R(\pi\epsilon_A, \phi_{\mathrm{B2}})R(\theta\epsilon_A, 0)\Big]R(\theta, 0) \end{aligned}$$

where the identity $R(2\pi, 3\phi_{\mathrm{B2}}) = -\mathbb{1} = R(\pi, \phi_{\mathrm{B2}} + \pi)R(\pi, \phi_{\mathrm{B2}} + \pi)$ was used. Let Q denote the quantity enclosed in square brackets, so that we may write $M_{\mathrm{B2}}(\theta, 0) = QU_T$. Observe that Q is precisely the form considered previously in N2. From our previous result, we may conclude $Q = \mathbb{1} + \mathcal{O}(\epsilon_A^3)$ and $M_{\mathrm{B2}}(\theta, 0) = R(\theta, 0) + \mathcal{O}(\epsilon_A^3)$. As a result, when $M_{\mathrm{B2}}(\theta, 0)$ is used in the place of the imperfect operation $M(\theta, 0)$ the effect of the systematic amplitude error is reduced. Note that errors for the B2 and N2 sequences follow equivalent paths on the Lie algebra in their respective interaction frames. In Fig. 7c, we plot the magnetization trajectory for a qubit under a B2 sequence with amplitude errors.

3. *Passband Behavior*

In some cases, it is convenient to have a passband pulse sequence that corrects for both addressing errors and for amplitude errors, as we saw with the Solovay–Kitaev sequences. The passband Wimperis sequence P2 is simply two

Solovay–Kitaev correction sequences in a row where the order of pulses is switched, $M_{P2}(\theta, 0) = M(2\pi, \phi_{P2})M(2\pi, -\phi_{P2})M(2\pi, -\phi_{P2})M(2\pi, \phi_{P2})M(\theta, 0)$, with $\phi_{P2} = \arccos(-\theta/8\pi)$. The switching of pulse order naturally removes the second-order error term. One may verify that this sequence works for both addressing and amplitude errors.

4. *Arbitrarily Accurate Trotter-Suzuki Sequences*

The Wimperis sequences rely on a certain symmetrical ordering of pulse sequence propagators to ensure that even-order Magnus expansion terms are eliminated. We may further improve the performance of these sequences by taking advantage of additional symmetries that cancel higher-order terms. In the following, we shall show how by using symmetric Trotter-Suzuki formulas [46,47,60] a family of arbitrarily accurate composite pulse sequences may be constructed [51,53]. The Lie algebraic picture along with the Magnus and BCH series will be important tools in this process.

a. Symmetrized Suzuki Formulas. Before discussing the particular form of these sequences, it is helpful to briefly mention a few important results regarding symmetric products of time-independent propagators [47]. Given a series of skew-Hermitian time-independent Hamiltonians $\{\tilde{H}_1, \tilde{H}_2, \ldots, \tilde{H}_m\}$ such that $\sum_i^m \tilde{H}_i = \tilde{H}_T$, the BCH expansion tells us

$$\prod_{i=1}^{m} \exp(\lambda \tilde{H}_i) = \exp\left(\lambda \tilde{H}_T + \sum_{n=2}^{\infty} \lambda^n \Omega_n\right) \tag{44}$$

where λ is a real parameter and the expansion terms Ω_n depend on the specific ordering of the sequence. If we choose to apply the operators in a time-symmetric manner such that $\exp(\lambda \tilde{H}_i) = \exp(\lambda \tilde{H}_{m+1-i})$, then the symmetry of the pulse removes all even-order terms. For symmetric products, we have

$$\prod_{\text{symmetric}} \exp(\lambda \tilde{H}_i) = \exp\left(\lambda \tilde{H}_T + \sum_{j=2}^{\infty} \lambda^{2j-1} \Omega_{2j-1}\right) \tag{45}$$

An important observation concerning the elimination of the remaining odd terms was made by Suzuki [47]. Provided that $\tilde{H}_i = p_i \tilde{H}_T + (p_i)^{2j-1} \tilde{H}_B$, where the coefficients p_i are real numbers, there exist certain choices of coefficients such that $\sum_i^m \tilde{H}_i = \tilde{H}_T$. This requires that $\sum_i^m p_i = 1$ and $\sum_i^m (p_i)^{2j-1} = 0$. The situation is considerably simplified if we restrict ourselves to sequences composed of just two kinds of propagators, $U_1 = \exp(\tilde{H}_1)$ and $U_2 = \exp(\tilde{H}_2)$. In this case the previous expression simplifies to $n_1 p_1 + n_2 p_2 = 1$ and $n_1 p_1^{2j-1} + n_2 p_2^{2j-1} = 0$, where the integers n_1 and n_2 are the number of U_1 and U_2 pulses required to

produce a sequence that is independent of H_B up to $\mathcal{O}(p^{2j+1})$. We solve for a set of coefficients by setting $p_2 = -2p_1$ and $n_2 = 1$, thus yielding $n_1 = 2^{2j-1}$ and $p_1 = 1/(2^{2j-1} - 2)$.

Combining these observations, if $W_{2j-2}(p)$ is a $(2j-2)$th approximation of $\exp(p\tilde{H}_T)$ and $\Omega_{2j-1} = p^{2j-1}\tilde{H}_B$ where $\tilde{H}_B$ is independent of p, then we can construct $W_{2j}(1)$ from the lower approximations, $W_{2j}(1) = (W_{2j-2}(p))^{2^{2j-2}} W_{2j-2}(-2p)(W_{2j-2}(p))^{2^{2j-2}}$. As a result, Suzuki formulas provide a path of producing higher-order sequences from a symmetric combination of lower-order sequences. Notice that the symmetric decomposition is used to keep the even-order terms zero.

b. Passband Behavior. In the following, we will seek to generalize the second-order passband sequence P2 to an arbitrarily accurate passband sequence P2j. Our goal is to develop a correction sequence $T_{2j}(k, \phi) = \exp(\mathrm{i}\theta\epsilon_A H_\mathrm{x}) + \mathcal{O}(\epsilon_A^{2j+1})$ that cancels the unwanted rotation of a $M(\theta, 0)$ operation.

When considering passband sequences, it is convenient to use rotation angles that are integer multiples of 2π. Let us define the triangular motif,

$$\begin{aligned} T_1(k, \phi) &= M(2k\pi, -\phi)M(2k\pi, \phi) \\ &= \exp(-\mathrm{i}4k\pi\epsilon_A \cos\phi H_\mathrm{x} - \mathrm{i}(2\pi k\epsilon_A)^2 \cos\phi \sin\phi H_\mathrm{z}) + O(\epsilon_A^3) \end{aligned} \tag{46}$$

Observe the passband sequence SK1 may now be written as $M_{\mathrm{SK1}}(\theta, 0) = T_1(1, \phi_{\mathrm{SK1}})M(\theta, 0)$ and where the phase ϕ_{SK1} is as defined previously. The remaining second-order term is odd with respect to ϕ, and is related to the vector cross-product on the Lie algebra. A second-order sequence may be constructed by combining two $T_1(k, \phi)$ terms so that the correction sequence is symmetric and the cross-product cancels. Let us define the symmetrized product

$$\begin{aligned} T_2(k, \phi) &= T_1(k, -\phi)T_1(k, \phi) \\ &= \exp(p\tilde{H}_T + p^3\tilde{H}_B) + \mathcal{O}(p^5) \end{aligned} \tag{47}$$

where the length $p = -(8k\pi/\theta)\cos\phi$, the target Hamiltonian $\tilde{H}_T = \mathrm{i}\theta\epsilon_A H_\mathrm{x}$, and $\tilde{H}_B = \epsilon_A^3\Omega_3/p^3$ is the remaining term we wish to cancel. Ω_3 is a function that depends on k and ϕ such that $\tilde{H}_B$ is a function of ϕ but not of the length scale k. For fixed ϕ and variable k, this makes H_B independent of p. Observe that the passband sequence P2 may now be written as $M_{\mathrm{P2}}(\theta, 0) = T_2(1, \phi_{\mathrm{P2}})M(\theta, 0)$, where again $\phi_{\mathrm{P2}} = \arccos(-\theta/8\pi)$.

Our strategy is to use a Suzuki formula to construct higher-order $T_4(k, \phi)$ (i.e., $T_{2j}(k, \phi)$ for $j = 2$), using a symmetric combination of $(n_1 = 8)$-many $\exp(\tilde{H}_1) = T_2(k, \phi)$ sequences and a single $\exp(\tilde{H}_2) = T_2(-2k, \phi)$ sequence, yielding

$$T_4(k, \phi) = \Big(T_2(k, \phi)\Big)^4 T_2(-2k, \phi)\Big(T_2(k, \phi)\Big)^4 \tag{48}$$

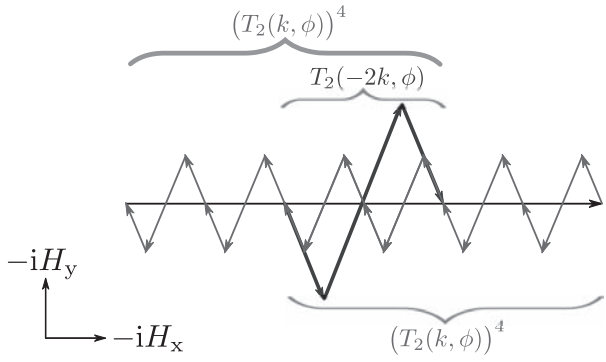

Figure 8. Vector path followed by P4 on the Lie algebra.

In order to produce required correction term, the parameters (k, ϕ) must be chosen such that $(n_1 - 2)p = 1$. The fourth-order passband sequence P4 is $M_{\mathrm{P4}}(\theta, 0) = T_4(1, \phi_{\mathrm{P4}})M(\theta, 0)$, where $\phi_{\mathrm{P4}} = \arccos(-\theta/48\pi)$. In Fig. 8, we plot the vector path followed by P4 on the Lie algebra. This result may be further generalized. To produce $T_{2j}(k, \phi)$ requires $(n_1 = 2^{2j-1})$-many $T_{2j-2}(k, \phi)$ sequences and a single $T_{2j-2}(-2k, \phi)$ sequence in the symmetric ordering

$$T_{2j}(k,\phi) = \Big(T_{2j-2}(k,\phi)\Big)^{2^{2j-2}} T_{2j-2}(-2k,\phi)\Big(T_{2j-2}(k,\phi)\Big)^{2^{2j-2}} \tag{49}$$

We then fix ϕ so that the first-order term cancels the unwanted rotation, yielding

$$\phi_{\mathrm{P}2j} = \arccos\left(-\frac{\theta}{2\pi f_j}\right) \tag{50}$$

where $f_j = (2^{2j-1} - 1)f_{j-1}$ and for the sequence P2j, $f_1 = 4$. Then the $2j$th-order passband sequence P2j is $M_{\mathrm{P}2j}(\theta, 0) = T_{2j}(1, \phi_{\mathrm{P}2j})M(\theta, 0)$.

The same method can be used to develop exclusively narrowband or broadband sequences called N2j and B2j, respectively [51]. This requires redefining the bottom recursion layer $T_2(k, \phi)$ to have either narrowband or broadband properties. For N2j, $f_1 = 2$ and $T_2(k, \phi) = T_1(k/2, \phi)T_1(k/2, -\phi)$. For B2$j$ $f_1 = 2$, but T_2 is slightly more complicated; when k is even $T_2(k, \phi) = T_1(k/2, -\phi)T_1(k/2, \phi)$ just like N2j, however, when k is odd and $T_2(k, \phi) = M(k\pi, \phi)M(k\pi, 3\phi)M(k\pi, 3\phi)$. In Fig. 9, we compare several of the generalized Trotter–Suzuki sequences to the ideal unitaries $U_T = R(\pi/2, 0)$ in the case of amplitude errors (top row) and $U_T = \mathbb{1}$ in the case of addressing errors on unaddressed qubits (bottom row).

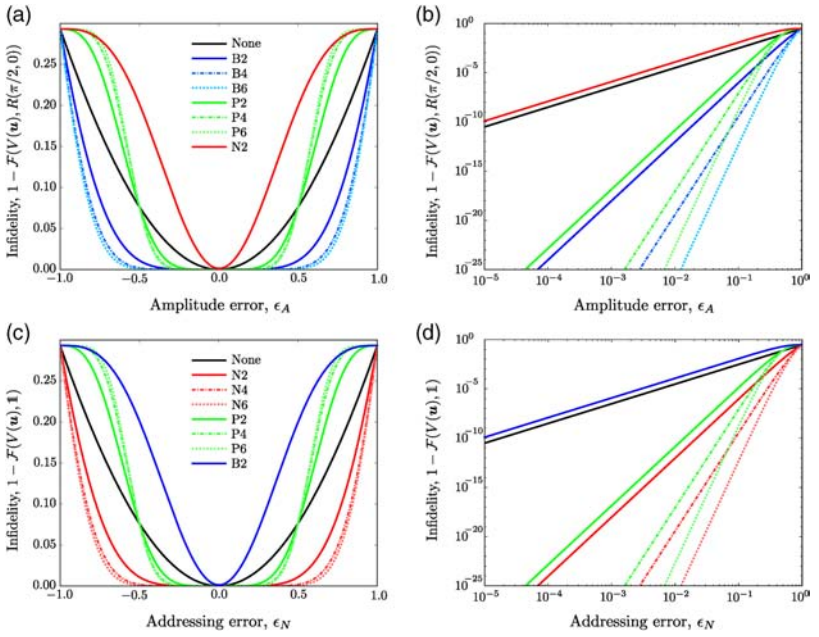

Figure 9. Infidelity of the Trotter–Suzuki sequences B2j, P2j, and N2j. (**a, b**) In the amplitude error model, $M(\theta, \phi) = M(\theta(1 + \epsilon_A), \phi)$ and $U_T = R(\pi/2, 0)$. (**c, d**) In the addressing error model on the unaddressed qubits $M(\theta, \phi) = M(\theta\epsilon_N, \phi)$ and $U_T = \mathbb{1}$, while on the addressed spins $R(\pi/2, 0)$ is applied. Each error model establishes a separate preferred interaction frame; when transformed into the appropriate pictures, the B2j and N2j sequences are homologous. The passband sequences P2j can correct both amplitude and addressing errors at the cost of reduced efficacy.

C. CORPSE

So far, the sequences considered here have been designed to correct systematic amplitude and addressing errors. The correction of errors arising from an inaccurate tuning of the control field are also of practical interest. The treatment of detuning errors is similar in principle to the error models already considered, however, in practice the construction of compensating sequences is complicated by the noncommutivity of the ideal Hamiltonian and the erroneous Hamiltonian generated by the control distortion $[\boldsymbol{u}(t) \cdot \boldsymbol{H}, \boldsymbol{\delta u}(t) \cdot \boldsymbol{H}] \neq 0$.

Fully compensating pulse sequences for detuning errors were originally studied by Tycko [61] and later generalized by Cummins and Jones into the humorously named ROTTEN (resonance offset tailoring to enhance nuition) [62] and CORPSE (compensating for off-resonance with a pulse sequence) [63,64] family

of sequences. Cummins and Jones initially derived the sequence using quaternion algebra to represent simple rotations, and optimized the angles to eliminate the first-order effects of the detuning error. The CORPSE family of sequences has found application in NMR [63] and SQUID [65] experiments. Here, we reexamine CORPSE using the techniques outlined in Section III.B.2.

CORPSE is a sequence that performs a compensated rotation about the H_x axis. Following Cummins and Jones, the sequence is constructed from three square pulses, which in the case of perfect resonance, induce rotations about the H_x, $-H_x$, and H_x axes, sequentially. The pulse sequence is parametrized by the piecewise constant control function

$$u_x(t) = \begin{cases} u_x & 0 \le t < t_1 \\ -u_x & t_1 \le t < t_2 \\ u_x & t_2 \le t \le \tau \end{cases} \tag{51}$$

where u_x is a constant H_x control amplitude and the t_j are times at which the field direction is switched. This construction is particularly amenable to analytic methods, as the ideal control Hamiltonian $H(t) = u_x(t)H_x$ commutes with itself at all times. In the absence of systematic detuning errors the control Hamiltonian produces the following ideal unitary evolution,

$$U(u_x(t')\mathbf{x}; t, 0) = \exp(-i\vartheta(t)H_x) = R(\vartheta(t), 0), \qquad \vartheta(t) = \int_0^t dt' u_x(t') \tag{52}$$

Over the entire time interval $0 \le t \le \tau$, the pulse sequence produces the gate $U_T = R(\theta, 0)$, where $\theta = \vartheta(\tau)$.

In the presence of an unknown detuning error, $\boldsymbol{\delta u} = \epsilon_D \mathbf{z}$, the rotation axis is lifted in the direction of the H_z axis on the Bloch sphere. A Magnus expansion may be used for the interaction frame propagator $U^I(\epsilon_D \mathbf{z}; \tau, 0)$, which produces the evolution generated by the systematic detuning error. Combining Eqs. (17) and (52) the first-order term is

$$\epsilon_D \Omega_1(\tau, 0) = -i\epsilon_D \int_0^\tau dt \cos(\vartheta(t))H_z + \sin(\vartheta(t))H_y \tag{53}$$

Direct integration yields:

$$\begin{aligned} \epsilon_D \Omega_1(\tau, 0) = &-\frac{i\epsilon_D}{u_x}[\sin(\theta_1)H_z + (1 - \cos(\theta_1))H_y] + \cdots \\ &+ \frac{i\epsilon_D}{u_x}[(\sin(\theta_1 - \theta_2) - \sin(\theta_1))H_z \\ &+ (\cos(\theta_1) - \cos(\theta_1 - \theta_2))H_y] + \cdots \\ &- \frac{i\epsilon_D}{u_x}[(\sin(\theta_1 - \theta_2 + \theta_3) - \sin(\theta_1 - \theta_2))H_z \\ &+ (\cos(\theta_1 - \theta_2) - \cos(\theta_1 - \theta_2 + \theta_3))H_y] \end{aligned} \tag{54}$$

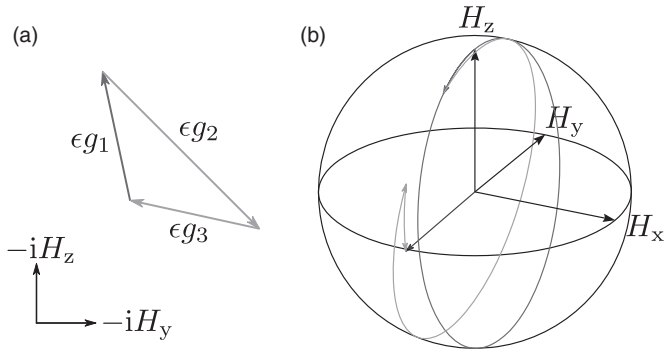

Figure 10. (**a**) Vector path followed by CORPSE on the Lie algebra, with the choice of parameters $n_1 = n_2 = n_3 = 0$. Each vector g_k corresponds to a term in Eq. (54). (**b**) Trajectory of a spin under a CORPSE sequence for $U_T = R(\pi/2, 0)$, with $n_1 = n_2 = 1$ and $n_3 = 0$ chosen to produce positive angles. The sequence is constructed of imperfect rotations of the form $M(\theta_k, 0) = \exp(-\mathrm{i}(\theta_k H_\mathrm{x} + \epsilon_D \theta_k H_\mathrm{z}))$, with $\epsilon_D = 0.2$.

where $\theta_k = \vartheta(t_k) - \vartheta(t_{k-1})$ are the effective rotation angles applied during the kth square pulse. At this point, we may interpret each of the terms of Eq. (54) as vectors on the dynamical Lie algebra. Figure 10a is a diagram of these vectors on $\mathfrak{su}(2)$. In order to eliminate the first-order expansion term, the rotation angles θ_k must be chosen so that the vectors must form a closed path.

Then by choosing the rotation angles to be

$$\begin{aligned}
\theta_1 &= 2\pi n_1 + \theta/2 - \arcsin\left(\sin(\theta/2)/2\right) \\
\theta_2 &= 2\pi n_2 - 2\arcsin\left(\sin(\theta/2)/2\right) \\
\theta_3 &= 2\pi n_3 + \theta/2 - \arcsin\left(\sin(\theta/2)/2\right)
\end{aligned} \tag{55}$$

where n_1, n_2, and n_3 are integers, we find that both $\epsilon_D \Omega_1(\tau, 0) = 0$ and $\theta = (\theta_1 - \theta_2 + \theta_3 \mod 2\pi)$. The extra factors of 2π are added so that the individual pulse rotation angles may be made positive. In principle, any choice of integers is sufficient to compose a first-order sequence, however, the choice $n_1 = n_2 = 1$ and $n_3 = 0$ minimizes the remaining second-order term while still producing a positive set of rotation angles [64]. The CORPSE family of sequences

$$\begin{aligned}
V(\boldsymbol{u}(t)) &= \exp(-\mathrm{i}(\theta_3 H_\mathrm{x} + \epsilon_D \theta_3 H_\mathrm{z}))\exp(-\mathrm{i}(-\theta_2 H_\mathrm{x} + \epsilon_D \theta_2 H_\mathrm{z})) \\
&\quad \times \exp(-\mathrm{i}(\theta_1 H_\mathrm{x} + \epsilon_D \theta_1 H_\mathrm{z})) \\
M_{\mathrm{C1}}(\theta, 0) &= M(\theta_3, 0) M(\theta_2, \pi) M(\theta_1, 0) = R(\theta, 0) + \mathcal{O}(\epsilon_D^2)
\end{aligned} \tag{56}$$

are fully compensating first-order sequences. In the presence of an unknown detuning error, a CORPSE sequence, $M_{\mathrm{C1}}(\theta, 0)$, may be implemented in the place of the simple rotation $R(\theta, 0)$ and the erroneous evolution is suppressed. In Fig. 10b,

we plot the magnetization trajectory for a qubit under a CORPSE sequence with detuning error $\epsilon_D = 0.2$.

1. *Arbitrarily Accurate CORPSE*

We turn our attention to sequences that compensate detuning errors to arbitrarily high order. Once again, the Solovay–Kitaev method may be used to construct higher-order sequences, now using CORPSE as the seed sequence. This problem was first studied by Alway and Jones [53]. Recall that in the Solovay–Kitaev method, one synthesizes a correction sequence B_{n+1} in two steps. First, one generates a propagator $P_{(n+1)z}(\xi)$ with an amplitude proportional to the leading-order error term. Second, the similarity transformation $U_T \Upsilon^\dagger$ is used so that $B_{n+1} = U_T \Upsilon^\dagger P_{(n+1)z}(\xi) \Upsilon U_T^\dagger$ cancels the leading error term of the seed sequence (see Eq. (35)). Equation (34) shows that the term $P_{(n+1)z}(\xi)$ may be constructed recursively using a product of first-order P_1s. Therefore, the Solvay-Kitaev method may be extended to correct detuning errors if (1) procedures for generating P_{1x}, P_{1y}, and P_{1z} using imperfect pulses have been found, and (2) when a method for applying the similarity transformation $U_T \Upsilon^\dagger$ using imperfect pulses has been identified. This task is complicated by the difficulty of generating inverse operations for imperfect pulses affected by detuning errors.

Earlier, the first-order P_1s were applied using a composite pulse sequence (see Eq. (37)). We employ a similar strategy here. Let

$$S_z(\alpha) = M(\alpha/2, \phi + \pi) M(\alpha/2, \phi) = \exp(-\mathrm{i}\alpha\epsilon H_\mathrm{z}) = P_{1z}(\alpha) \tag{57}$$

Then we may apply $P_{1z}(\alpha)$ by implementing the sequence $S_z(\alpha)$ instead. What remains is to develop sequences that apply $P_{1x}(\alpha)$ and $P_{1y}(\alpha)$. Observe that if it were possible to perform ideal rotations (where $R^\dagger(\theta, \phi) = R(\theta, \phi + \pi)$), then one could easily implement $S_x(\alpha) = R(\pi/2, \pi/2) S_z(\alpha) R^\dagger(\pi/2, \pi/2)$ and $S_y(\alpha) = R^\dagger(\pi/2, 0) S_z(\alpha) R(\pi/2, 0)$ in the place of $P_{1x}(\alpha)$ and $P_{1y}(\alpha)$. However, in the presence of systematic detuning errors, we may not apply this transformation using a simple imperfect pulse since $M^\dagger(\theta, \phi) \neq M(\theta, \phi + \pi)$. We may avoid this complication by using a CORPSE sequence to approximate the transformation to sufficient accuracy. We use the first-order CORPSE sequence, $M_{\mathrm{C1}}(\theta, \phi)$ to implement the target operation $U_T = R(\theta, \phi)$. Then we may write

$$\begin{aligned} S_x(\alpha) &= M_{\mathrm{C1}}(\pi/2, \pi/2) S_z(\alpha) M_{\mathrm{C1}}(\pi/2, 3\pi/2) \\ &= \exp(-\mathrm{i}\alpha\epsilon H_\mathrm{x}) + \mathcal{O}(\epsilon^2) = P_{1x}(\alpha) \end{aligned} \tag{58}$$

and

$$S_y(\alpha) = M_{\mathrm{C1}}(\pi/2, \pi) S_x(\alpha) M_{\mathrm{C1}}(\pi/2, 0) = \exp(-\mathrm{i}\alpha\epsilon H_\mathrm{y}) + \mathcal{O}(\epsilon^2) = P_{1y}(\alpha) \tag{59}$$

Furthermore, by careful choice of θ and ϕ, we can implement $P_{1\eta}(\alpha)$ for any axis η about any angle α. Following the Solovay–Kitaev method, we can then construct $P_{jz}(\xi)$ to any order j.

What remains is to implement the similarity transformation by $U_T \Upsilon^\dagger$. However, we note that the available approximate rotations $M_{\mathrm{C1}}(\theta, \phi) = R(\theta, \phi) + \mathcal{O}(\epsilon_D)$ are only accurate to first order. Hence, if we were to attempt to apply a similarity transformation on a higher-order $P_{jz}(\xi)$ term using CORPSE sequences, additional second-order errors would be introduced. This difficulty may be avoided by applying the appropriate rotation at the level of the first-order P_1 operations. As an instructive example, we work through the process for the second-order correction. The correction sequences may be constructed in a rotated coordinate system, determined by the basis transformation $H'_\mu = U_T \Upsilon^\dagger H_\mu \Upsilon U_T^\dagger$ for $\mu \in \{\mathrm{x}, \mathrm{y}, \mathrm{z}\}$. One may calculate four rotations $R(\theta_{\pm\mu'}, \phi_{\pm\mu'})$, that map the H_z axis to the $H_{\pm\mathrm{x}'}$ and $H_{\pm\mathrm{y}'}$ axes $H_{\pm\mu'} = R(\theta_{\pm\mu'}, \phi_{\pm\mu'}) H_\mathrm{z} R^\dagger(\theta_{\pm\mu'}, \phi_{\pm\mu'})$ and also $P_{1\pm\mu'}(\alpha) = R(\theta_{\pm\mu'}, \phi_{\pm\mu'}) P_{1z}(\alpha) R^\dagger(\theta_{\pm\mu'}, \phi_{\pm\mu'})$. This transformation may also be applied using a first-order CORPSE sequence, because the resulting error is absorbed into the second-order error term in $P_{1\pm\mu'}(\alpha)$. Once transformed terms have been obtained, the correction sequence may be constructed in the usual manner

$$
\begin{aligned}
B_2 = P_{2z'}(\xi) &= P_{1x'}(-\sqrt{\xi}) P_{1y'}(-\sqrt{\xi}) P_{1x'}(\sqrt{\xi}) P_{1y'}(\sqrt{\xi}) \\
&= M_{\mathrm{C1}}(\theta_{-x'}, \phi_{-x'}) P_{1z}(\sqrt{\xi}) M_{\mathrm{C1}}(\theta_{-x'}, \phi_{-x'} + \pi) M_{\mathrm{C1}}(\theta_{-y'}, \phi_{-y'}) P_{1z}(\sqrt{\xi}) \\
&\quad \times M_{\mathrm{C1}}(\theta_{-y'}, \phi_{-y'} + \pi) M_{\mathrm{C1}}(\theta_{x'}, \phi_{x'}) P_{1z}(\sqrt{\xi}) M_{\mathrm{C1}}(\theta_{x'}, \phi_{x'} + \pi) \\
&\quad \times M_{\mathrm{C1}}(\theta_{y'}, \phi_{y'}) P_{1z}(\sqrt{\xi}) M_{\mathrm{C1}}(\theta_{y'}, \phi_{y'} + \pi)
\end{aligned}
$$

We can then define a second-order CORPSE sequence as $M_{\mathrm{C2}}(\theta, 0) = B_2 M_{\mathrm{C1}}(\theta, 0) = R(\theta, 0) + \mathcal{O}(\epsilon_D^3)$. One can then continue using Solvay-Kitaev techniques to remove the detuning error to all orders.

2. *Concatenated CORPSE: Correcting Simultaneous Errors*

So far, we have considered the problem of quantum control in the presence of a single systematic error, while in a real experiment several independent systematic errors may affect the controls. In many situations one error dominates the imperfect evolution; it is appropriate in these cases to use a compensating sequence to suppress the dominant error. However, it is also important to consider whether a sequence reduces the sensitivity to one type of error at the cost of increased sensitivity to other types of errors [64]. Such a situation may occur if an error model couples two error sources. Consider a set of control functions $\{u_\mu(t)\}$ where each control is deformed by two independent systematic errors. A general

two-parameter error model for the control $v_\mu(t) = f_\mu[\boldsymbol{u}(t); \epsilon_i, \epsilon_j]$ may be formally expanded as

$$f_\mu[\boldsymbol{u}(t); \epsilon_i, \epsilon_j] = f_\mu[\boldsymbol{u}(t); 0, 0] + \epsilon_i \frac{\partial}{\partial \epsilon_i} f_\mu[\boldsymbol{u}(t); 0, 0] + \epsilon_j \frac{\partial}{\partial \epsilon_j} f_\mu[\boldsymbol{u}(t); 0, 0] + 2\epsilon_i \epsilon_j \frac{\partial^2}{\partial \epsilon_i \partial \epsilon_j} f_\mu[\boldsymbol{u}(t); 0, 0] + \mathcal{O}(\epsilon_i^2 + \epsilon_j^2) \tag{60}$$

In practice, we need only concern ourselves with the first few expansion terms, because in most physically relevant error models the higher-order derivatives are identically zero. Following the same reasoning employed in Section II, we may decompose the imperfect propagator as $V(\boldsymbol{u}(t)) = U(\boldsymbol{u}(t))U^I(\boldsymbol{v}(t) - \boldsymbol{u}(t))$, where $U(\boldsymbol{u}(t))$ is the ideal propagation in the absence of errors and the interaction frame propagator $U^I(\boldsymbol{v}(t) - \boldsymbol{u}(t))$ represents the evolution induced by the systematic errors. Formally $U^I(\boldsymbol{v}(t) - \boldsymbol{u}(t))$ may be studied using a Magnus expansion, however, this method is usually impeded by the complexity of the Magnus series. The determination of sequences that compensate simultaneous errors is currently an unresolved problem, although some progress has been made by considering concatenated pulse sequences [31]. As an example relevant to an NMR quantum computer, we now study error models where two systematic errors occur simultaneously and show that these errors can be compensated by concatenation of pulse sequences.

a. Simultaneous Amplitude and Detuning Errors. When studying the control of qubits based on coherent spectroscopy methods, it is natural to consider situations where systematic errors in the field amplitude and tuning are simultaneously present. From the NMR control Hamiltonian Eq. (9) it is straightforward to derive the error model, $v_{\mathrm{x/y}} = u_{\mathrm{x/y}}(t)(1 + \epsilon_A)$ and $v_{\mathrm{z}} = u_{\mathrm{z}}(t) + \epsilon_D$. In this case, the independent amplitude and detuning errors are decoupled and the parameters ϵ_A and ϵ_D do not affect the same control.

b. Simultaneous Pulse-Length and Detuning Errors. Likewise, simultaneous errors in the pulse length and field tuning may occur. Again, it is simple to derive the joint error model, $v_{\mathrm{x/y}} = u_{\mathrm{x/y}}(t)(1 + \epsilon_T)$ and $v_{\mathrm{z}} = (u_{\mathrm{z}}(t) + \epsilon_D)(1 + \epsilon_T)$. Unlike the previous case, this error model couples the parameters ϵ_T and ϵ_D, because they both effect the H_z control function.

It is sometimes possible to produce a sequence that compensates two simultaneous errors by pulse sequence concatenation. Recall that the Wimperis sequence B2 is a second-order compensation sequence for both amplitude and pulse-length errors. However, if only detuning errors are present, then the response of a B2 sequence to pure detuning errors is similar to that of a native pulse Similarly, a CORPSE sequence would eliminate the first-order term produced by the detuning offsets but not correct amplitude errors. The sequence B2CORPSE corrects both errors *independently* by concatenating the B2 and CORPSE sequences.

B2CORPSE is composed of three B2 subsequences that form a larger CORPSE sequence

$$M_{\mathrm{B2C1}}(\theta, 0) = M_{\mathrm{B2}}(\theta_3, 0) M_{\mathrm{B2}}(\theta_2, \pi) M_{\mathrm{B2}}(\theta_1, 0) \tag{61}$$

where the angles $\{\theta_1, \theta_2, \theta_3\}$ are given in Eq. (55). At the lower level of concatenation, B2 sequences are used to synthesize rotations robust to pure amplitude or pulse-length errors, whereas on the higher level the CORPSE construction compensates pure detuning errors. Figure 11a–d are plots of the infidelity of plain pulses, and the CORPSE, B2, and B2CORPSE sequences in the presence of simultaneous amplitude and detuning errors. Similarly, Fig. 11e–h are infidelity plots for simultaneous pulse-length and detuning errors. As expected, the CORPSE sequences improve the accuracy of gates with respect to detuning errors, but offers little improvement against either amplitude or pulse length errors. Unsurprisingly, this behavior is inverted for the B2 sequences. The B2CORPSE sequence performs well for either amplitude/pulse-length or detuning errors; in the presence of simultaneous errors the performance diminishes, yet the fidelity of the applied gate is still vastly improved over uncompensated pulses.

D. Shaped Pulse Sequences

Thus far, we have considered sequences composed of control functions $u_\mu(t)$, which are piecewise constant over the pulse interval. This construction is particularly convenient from a sequence design perspective, although in practice instrumental shortcomings will frequently distort the pulse profile. Also, in some applications, the rectangular profile is nonideal. For example, in the frequency domain, the square pulse corresponds to a sinc function whose local maxima may complicate the control of certain systems. Finally, we note that in some systems, such as in superconducting Josephson junction qubits, bandwidth requirements forbid the sudden switching of control fields (i.e., place a limit on the derivative $|\dot{u}_\mu| \leq \dot{u}_\mu^{\mathrm{MAX}}$). In these cases, it is desirable to consider shaped pulse sequences composed by a set of continuous differentiable control functions [66]. In the present chapter, we shall only consider shaped pulse sequences, which are also fully compensating (class A), and therefore appropriate for use in a quantum processor. Specifically, we study shaped pulse sequences that also compensate systematic errors. We shall see that the additional flexibility admitted by shaped pulses frequently produces superior sequences.

Once given a pulse waveform, we may verify that it is compensating for a particular error model by computing the Magnus expansion in the appropriate interaction frame; however, we emphasize that these methods require the evaluation of successive nested integrals (e.g., Eq. (15)) and are difficult to analytically implement beyond the first few orders [67]. Furthermore, the inverse problem (solving for the control functions) is especially difficult except in the most simple

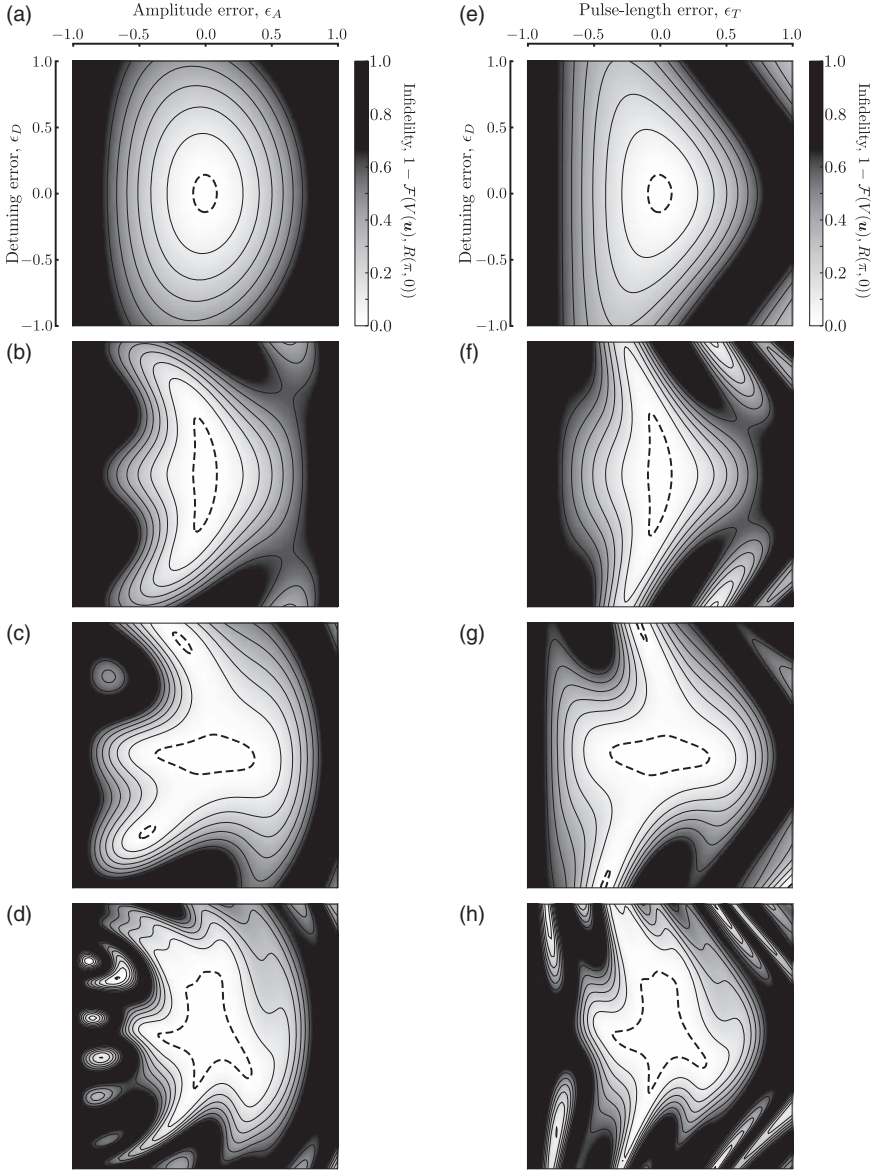

Figure 11. Infidelity of (**a, e**) plain pulses; (**b, f**) CORPSE; (**c, g**) B2; and (**d, h**) a concatenated B2CORPSE sequence in the presence of simultaneous amplitude and detuning (left column) and pulse-length and detuning (right column) errors. The target rotation is $U_T = R(\pi, 0)$. The dashed contour corresponds to an infidelity of 0.01, while the remaining contours are plotted at 10% intervals.

cases. For this reason, various numerical optimization methods have become popular, including gradient-accent techniques, optimal control methods [68–70], and simulated annealing [71,72]. Methods that use elements of optimal-control theory merit special attention; in recent years the GRAPE [73,74] and Krotov algorithms have been especially successful in pulse design, and has been applied to NMR [68], trapped ions [75], and ESR [76]. The main advantage of the GRAPE algorithm is an efficient estimation of the gradient of the fidelity as a function of the controls, which then enables optimization via a gradient-accent method. A recent review of these methods may be found in Refs [77,78].

To demonstrate the relative performance of shaped sequences, we consider the continuous analogs of the CORPSE sequence that modulate $u_x(t)$ to compensate detuning errors. From Eq. (53) observe that the first-order compensation condition $\epsilon_D \Omega_1(\tau, 0) = 0$ is met when $\int_0^\tau dt \cos(\vartheta(t)) = \int_0^\tau dt \sin(\vartheta(t)) = 0$. What remains is to solve for a set of control functions $u_x(t)$ that generate the target operation U_T while remaining robust to the detuning error. One popular scheme is to decompose the control functions as a Fourier series [72,79] over the pulse interval

$$u_x(t) = \omega \sum_{n=0}^{\infty} a_n \cos\left(n\omega\left(t - \frac{\tau}{2}\right)\right) + b_n \sin\left(n\omega\left(t - \frac{\tau}{2}\right)\right), \quad \omega = \frac{2\pi}{\tau} \tag{62}$$

This has the advantage of specifying the controls using only a few expansion parameters $\{a_n\}$ and $\{b_n\}$. Also, the series may be truncated to avoid high-frequency control modulations that are incompatible with some control systems. Moreover, by choosing each of the expansion terms $b_n = 0$, the resultant sequence may be made symmetric with respect to time reversal. We note that not all compensating sequences completely eliminate the first-order error term; in some sequences the leading order errors are highly suppressed rather than completely eliminated. This behavior is more common in sequences obtained from numerical methods.

Historically, the first class A shaped pulses developed belonged to the U-BURP (band-selective, uniform response, pure-phase) family designed by Geen and Freeman [25,72], using simulated-annealing, and gradient decent methods. Soon after, Abramovich and Vega attacked the same problem using approximation methods based on Floquet theory [80]. These sequences are designed to correct detuning errors over an extremely large range; however, they fail to completely eliminate the leading-order error terms. In the design of compensating sequences for quantum computing, the emphasis has been on the synthesis of composite rotations of extraordinary accuracy over a narrow window of errors. More recently, Steffen and Koch considered shaped Gaussian modulated controls specially designed for superconducting qubit manipulations [81]. Pryadko and Sengupta also derived a family of sequences ($S_1(\phi_0)$,$S_2(\phi_0)$,$Q_1(\phi_0)$,$Q_2(\phi_0)$) using a semianalytic method based on the Magnus expansion and average Hamiltonian theory [67,82]. By design, these sequences eliminate the leading-order error terms in a manner similar to the square-pulse sequences previously discussed.

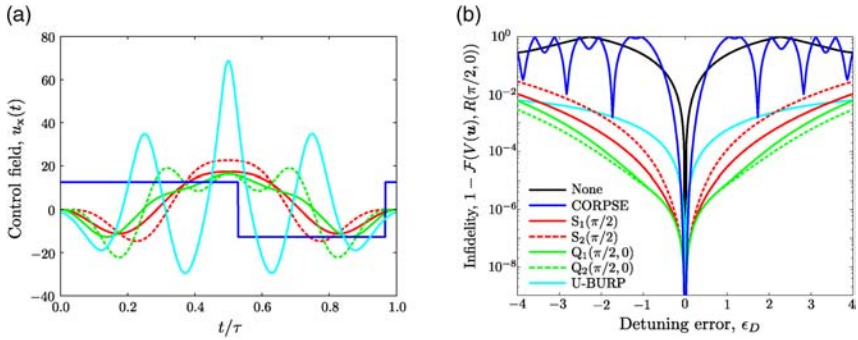

Figure 12. (**a**) Control function $u_x(t)$ for various pulse sequences designed to compensate systematic detuning errors. (**b**) Performance of several shaped pulses over a wide detuning range.

It is interesting to compare the performance of shaped sequences to a sequence of square pulses, such as CORPSE. Many of these sequences compensate detuning errors by modulating the amplitude of the control function $u_x(t)$. In Fig. 12a, pulse shapes are given for CORPSE, U-BURP, $S_1(\pi/2)$, $S_2(\pi/2)$, $Q_1(\pi/2)$, and $Q_2(\pi/2)$ sequences that implement the target operation $U_T = R(\pi/2, 0)$. The relative performance of these sequence over a wide range of systematic detuning error is given in Fig. 12b. Clearly, shaped pulses outperform CORPSE over a wide range of field tunings; however, for very small detunings, CORPSE has more favorable scaling behavior. Figure 13a and b show the behavior of the shaped pulse $S_1(\pi/2)$ as trajectories on the Lie algebra and on the Bloch sphere, respectively.

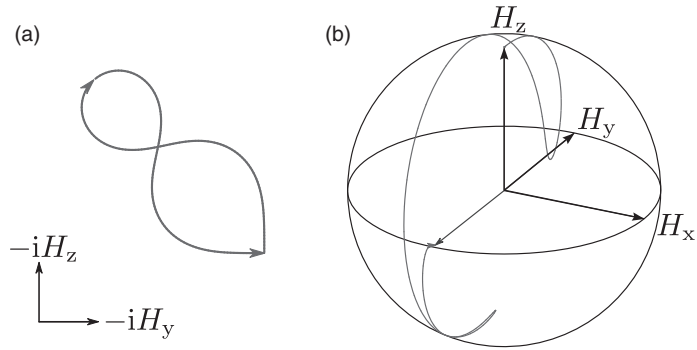

Figure 13. (**a**) Vector path on the Lie algebra traced out by the interaction frame Hamiltonian $H^I(t) = \epsilon_D H_z^I(t)$ for the shaped sequence $S_1(\pi/2)$. (**b**) Magnetization trajectory for a qubit under an $S_1(\pi/2)$ sequence for the target operation $U_T = R(\pi/2, 0)$, for the exceptionally large detuning error $\epsilon_D = 1$.

V. COMPOSITE PULSE SEQUENCES ON OTHER GROUPS

We have studied sequences that compensate imperfect single-qubit rotations (i.e., operations that form a representation of the group $\mathsf{SU}(2)$). Another class of problems of practical and fundamental interest is the design of sequences for other Lie groups, such as the group of n-qubit operations $\mathsf{SU}(2^n)$ [50]. Several compensating sequences exist for multi-qubit gates [57,58,83]. In general, these sequences rely on operations that form an $\mathsf{SU}(2)$ subgroup to perform compensation in a way analogous to the one-qubit case and is the topic of this section.

We note the design of compensating pulse sequences that do not rely on an $\mathsf{SU}(2)$ or $\mathsf{SO}(3)$ subgroup is a largely unexplored topic, and is an interesting subject for future study. For many cases, we can determine which errors can be compensated by examining the algebra [11], but it is unclear what the natural compensating sequences are for groups that are not equivalent to rotations in three dimensions.

A. Compensated Two-Qubit Operations

Thus far, we have shown how compensating sequences may be used to correct systematic errors in arbitrary one-qubit operations. Universal quantum computation also requires accurate two-qubit gates. The study of two-qubit compensating sequences is therefore of great fundamental and practical interest. In this section, we study two-qubit operations using Lie theoretic methods. The Cartan decomposition of the dynamical Lie algebra will be central to this approach. We begin by studying the properties and decompositions of the Lie group and its associated algebra. Then we consider systematic errors in two-qubit gates derived from the Ising interaction, and show how the Cartan decomposition may be used to construct compensating sequences.

Any two-qubit Hamiltonian (up to a global phase) may be written in the form

$$H(t) = \sum_{\mu} \sum_{\nu} u_{\mu\nu}(t) H_{\mu\nu} \tag{63}$$

where the controls are represented in the product-operator basis [84], corresponding to the control Hamiltonians $H_{\mu\nu} = 2H_\mu \otimes H_\nu$, where $H_1 = \frac{1}{2}\mathbb{1}$ and the indices μ, ν run over $H_\mu \in \{H_1, H_x, H_y, H_z\}$. As a matter of convention, we exclude the term proportional to the identity $H_{11} = \frac{1}{2}\mathbb{1} \otimes \mathbb{1}$ since it generates an unimportant global phase and otherwise does not contribute to the dynamics; it is implied in the following equations that this term never appears. The product-operator representation is particularly convenient because each control Hamiltonian is orthogonal under the Hilbert–Schmidt inner product, $\langle H_{\mu\nu}, H_{\rho\sigma} \rangle = \delta_{\mu,\rho}\delta_{\nu,\sigma}$. The family of all possible solutions to a control equation, for example, Eq. (1) with the Hamiltonian Eq. (63), forms a representation of the special unitary group $\mathsf{SU}(4)$. This

group contains all possible single-qubit (local) operations that may be applied to each qubit among the pair as well as all two-qubit (nonlocal) operations.

1. *Cartan Decomposition of Two-Qubit Gates*

Associated with the group $\mathsf{SU}(4)$ is the corresponding Lie algebra $\mathfrak{su}(4) = \bigoplus_{\mu\nu} \mathrm{span}\{-\mathrm{i}H_{\mu\nu}\}$ excluding H_{11} (including H_{11} would make the group $\mathsf{U}(4)$). Consequently, $\mathfrak{su}(4)$ is the algebra of four-dimensional traceless skew-Hermitian matrices. Observe that $\mathfrak{su}(4)$ may be decomposed as $\mathfrak{su}(4) = \mathfrak{k} \oplus \mathfrak{m}$, where

$$\mathfrak{k} = \mathfrak{su}(2) \oplus \mathfrak{su}(2) = \mathrm{span}\{-\mathrm{i}H_{\mathrm{x1}}, -\mathrm{i}H_{\mathrm{y1}}, -\mathrm{i}H_{\mathrm{z1}}, -\mathrm{i}H_{\mathrm{1x}}, -\mathrm{i}H_{\mathrm{1y}}, -\mathrm{i}H_{\mathrm{1z}}\}$$
$$\mathfrak{m} = \mathrm{span}\{-\mathrm{i}H_{\mathrm{xx}}, -\mathrm{i}H_{\mathrm{xy}}, -\mathrm{i}H_{\mathrm{xz}}, -\mathrm{i}H_{\mathrm{yx}}, -\mathrm{i}H_{\mathrm{yy}}, -\mathrm{i}H_{\mathrm{yz}}, -\mathrm{i}H_{\mathrm{zx}}, -\mathrm{i}H_{\mathrm{zy}}, -\mathrm{i}H_{\mathrm{zz}}\}$$

It may be verified that $[\mathfrak{k}, \mathfrak{k}] \subseteq \mathfrak{k}$, $[\mathfrak{m}, \mathfrak{k}] = \mathfrak{m}$, and $[\mathfrak{m}, \mathfrak{m}] \subseteq \mathfrak{k}$. Therefore, the decomposition $\mathfrak{k} \oplus \mathfrak{m}$ is a Cartan decomposition of the algebra $\mathfrak{su}(4)$. Also, the subalgebra $\mathfrak{a} = \mathrm{span}\{-\mathrm{i}H_{\mathrm{xx}}, -\mathrm{i}H_{\mathrm{yy}}, -\mathrm{i}H_{\mathrm{zz}}\}$ is a maximal abelian subalgebra and $\mathfrak{a} \subset \mathfrak{m}$. Therefore, $\mathfrak{a}$ is a Cartan subalgebra. This admits the decomposition $U = K_2 A K_1$ for any element $U \in \mathsf{SU}(4)$. The operators

$$K_j = \exp\left(-\mathrm{i} \sum_{\mu \in \{\mathrm{x,y,z}\}} \alpha_{\mu 1}^{(j)} H_{\mu 1} + \alpha_{1\mu}^{(j)} H_{1\mu}\right) \tag{64}$$

are in the subgroup $\mathrm{e}^{\mathfrak{k}} = \mathsf{SU}(2) \otimes \mathsf{SU}(2)$ comprising all single-qubit operations for both qubits, whereas the operator

$$A = \exp\left(-\mathrm{i} \sum_{\mu \in \{\mathrm{x,y,z}\}} \alpha_{\mu\mu} H_{\mu\mu}\right) \tag{65}$$

is in the abelian group $\mathrm{e}^{\mathfrak{a}} = \mathsf{T}^3$, isomorphic to the 3-torus, generated by the two-qubit interaction terms H_{xx}, H_{yy}, and H_{zz}. In analogy with the Euler decomposition, the parameters $\alpha_{\mu\nu}$ may be regarded as rotation angles. This construction is a KAK Cartan decomposition for the propagator U, and may be used as a framework for a pulse sequence to generate any arbitrary two-qubit operation. Furthermore, if the operators K_2, A, and K_1 may be implemented using a compensating pulse sequence, robust for a given error model, then their product will also be a compensating sequence.

2. *Operations Based on the Ising Interaction*

We seek a method for implementing an arbitrary gate $A \in \mathrm{e}^{\mathfrak{a}}$ using a two-qubit coupling interaction. To be specific, we consider an NMR quantum computer of two heteronuclear spin qubits coupled by an Ising interaction. It is well known

that propagators generated by the Ising interaction and single-qubit rotations are universal for SU(4) [85]; for completeness we explicitly show how arbitrary gates may be synthesized using the KAK form. Under the assumption of the qubits can be spectrally distinguished due to large differences in Larmor frequencies, the system Hamiltonian takes the form

$$H(t) = \left(\sum_{\mu \in \{\mathrm{x},\mathrm{y},\mathrm{z}\}} u_{\mu 1}(t) H_{\mu 1} + u_{1\mu}(t) H_{1\mu} \right) + u_{\mathrm{zz}}(t) H_{\mathrm{zz}} \tag{66}$$

where the controls $u_{\mu 1}(t)$ and $u_{1\mu}(t)$ are applied by the appropriate rf fields and $u_{\mathrm{zz}}(t) = 2\pi J(t)$ is the strength of the spin–spin coupling interaction. In some cases, it is useful to manipulate the strength of the scalar coupling $J(t)$ (e.g., by using spin decoupling techniques) [25]. We consider the simpler case of constant Ising couplings, and also assume that it is possible to apply hard pulses, where rf coupling amplitude greatly exceeds J, and the spin–spin coupling may be considered negligible. In terms of resource requirements for the quantum computer, this implies that single-qubit operations are fairly quick, whereas two-qubit operations driven by the Ising coupling are much slower.

Consider the propagators $U_{\mu\mu}(\alpha) = \exp(-\mathrm{i}\alpha H_{\mu\mu}) \in \mathrm{e}^{\mathfrak{a}}$. Let us define the one-qubit rotation operators $R_1(\theta, \phi) = R(\theta, \phi) \otimes \mathbb{1}$ and $R_2(\theta, \phi) = \mathbb{1} \otimes R(\theta, \phi)$. In the absence of applied rf fields, the system evolves according to $U_{\mathrm{zz}}(\theta_{\mathrm{zz}})$, where $\theta_{\mathrm{zz}} = u_{\mathrm{zz}} \Delta t$ and Δt is the duration of the free-precession interval. Observe that for

$$\begin{aligned} K_{\mathrm{x}} &= R_1(\pi/2, 0) R_2(\pi/2, 0) = \exp(-\mathrm{i}\pi/2(H_{\mathrm{x}1} + H_{1\mathrm{x}})) \\ K_{\mathrm{y}} &= R_1(\pi/2, \pi/2) R_2(\pi/2, \pi/2) = \exp(-\mathrm{i}\pi/2(H_{\mathrm{y}1} + H_{1\mathrm{y}})) \end{aligned} \tag{67}$$

$U_{\mathrm{xx}}(\alpha) = K_{\mathrm{y}} U_{\mathrm{zz}}(\alpha) K_{\mathrm{y}}^{\dagger}$ and $U_{\mathrm{yy}}(\alpha) = K_{\mathrm{x}}^{\dagger} U_{\mathrm{zz}}(\alpha) K_{\mathrm{x}}$. Because the group $\mathrm{e}^{\mathfrak{a}}$ is abelian, then any arbitrary group element A specified by the decomposition angles $\{\alpha_{\mathrm{xx}}, \alpha_{\mathrm{yy}}, \alpha_{\mathrm{zz}}\}$, may be produced by the product $A = U_{\mathrm{xx}}(\alpha_{\mathrm{xx}}) U_{\mathrm{yy}}(\alpha_{\mathrm{yy}}) U_{\mathrm{zz}}(\alpha_{\mathrm{zz}})$. Then any $U = K_2 A K_1 \in \mathrm{SU}(4)$ may be produced using single-qubit rotations and the Ising interaction.

a. Systematic Errors in Ising Control. In practice, systematic errors introduced by experimental imperfections prohibit the application of perfect two-qubit gates. In the case of gates produced by the Ising interaction, the errors may arise from several sources, such as experimental uncertainty in the strength of the coupling J. It is, therefore, desirable to design sequences that implement accurate Ising gates over a range of coupling strengths. The error model in this case is similar to the case of amplitude errors; the control u_{zz} is replaced by the imperfect analogue $v_{\mathrm{zz}} = u_{\mathrm{zz}}(1 + \epsilon_J)$ where the parameter ϵ_J is proportional to the difference between the nominal (measured) and actual coupling strengths. For now we assume

the remaining controls are error free. In correspondence, the perfect propagators $U_{zz}(\theta_{zz})$ are replaced by $V_{zz}(\theta_{zz}) = U_{zz}(\theta_{zz}(1+\epsilon_J))$.

Jones was the first to study compensating pulse sequences for the Ising interaction [55,57], and proposed sequences closely related to the Wimperis sequences studied in Section IV.B. Here, we demonstrate that these sequences are easily derived using Lie algebraic techniques. Observe that several subalgebras are contained in $\mathfrak{su}(4)$, for instance $\mathfrak{j} = \mathrm{span}\{-iH_{x1}, -iH_{yz}, -iH_{zz}\}$, which are representations of $\mathfrak{su}(2)$. Furthermore, if it is feasible to produce any imperfect propagator in the group $\mathsf{J} = e^{\mathfrak{j}}$, then the compensating sequences discussed in Section IV may be reused for this system.

This strategy can be implemented using accurate one-qubit rotations. For example, let

$$\mathcal{R}(\theta,\phi) = R_1^\dagger(\phi,0)U_{zz}(\theta)R_1(\phi,0) = \exp(-i\theta(\cos\phi H_{zz} + \sin\phi H_{yz})) \quad (68)$$

Also, let us define the imperfect rotation $\mathcal{M}(\theta,\phi) = R_1^\dagger(\phi,0)V_{zz}(\theta)R_1(\phi,0) = \mathcal{R}(\theta(1+\epsilon_J),\phi)$. The two-qubit unitaries $\mathcal{R}(\theta,\phi)$ are isomorphic to single-qubit rotations $\mathcal{R}(\theta,\phi)$ and Jones used this similarity to construct an alternative sequence we refer to as B2-J [57,58]:

$$\begin{aligned}\mathcal{M}_{\text{B2-J}}(\theta,0) &= \mathcal{M}(\pi,\phi)\mathcal{M}(2\pi,3\phi)\mathcal{M}(\pi,\phi)\mathcal{M}(\theta,0)\\ &= R_1^\dagger(\phi,0)U_{zz}(\pi(1+\epsilon_J))R_1(\phi,0)\, R_1^\dagger(3\phi,0)U_{zz}(2\pi(1+\epsilon_J))\\ &\quad\times R_1(3\phi,0)R_1^\dagger(\phi,0)U_{zz}(\pi(1+\epsilon_J))R_1(\phi,0)\, U_{zz}(\theta(1+\epsilon_J))\\ &= U_{zz}(\theta) + \mathcal{O}(\epsilon_J^3) \end{aligned} \quad (69)$$

where again $\phi = \arccos(-\theta/4\pi)$. If the sequence B2-J is used in place of the simple Ising gate $U_{zz}(\theta)$ then the first- and second-order effects of the systematic error are eliminated. In this manner, any number of sequences designed for operations in $\mathsf{SU}(2)$ may be mapped into sequences that compensate Ising gates, including the higher-order Trotter–Suzuki sequences, which produce gates at an arbitrary level of accuracy. However, we note that because two-qubit gates occur so slowly, the practical utility of very long sequences is not clear, especially in systems where the two-qubit gate time is comparable to the qubit coherence lifetime. Substantial improvements in the minimum time requirements may be possible with shaped pulse sequences or using time-optimal control methods [86].

In this method, accurate one-qubit gates are used to transform inaccurate Ising gates into a representation of $\mathsf{SU}(2)$. Naturally, it is unimportant which qubit among the pair is rotated to perform this transformation (i.e., the subalgebra $\mathfrak{j}' = \mathrm{span}\{-iH_{1x}, -iH_{zy}, -iH_{zz}\}$ would serve just as well). Given a control with a systematic error and a perfect rotation operator that transforms the control

Hamiltonian H_μ to an independent Hamiltonian H_ν, it is possible to perform compensation if H_μ, and H_ν generate a representation of $\mathfrak{su}(2)$ [58].

b. Correcting Simultaneous Errors. Accurate single-qubit gates are required to compensate errors in the Ising coupling by transforming Ising gates into the larger dynamical Lie group. If accurate single-qubit operations are not available, then propagators of the form Eq. (68) can no longer be reliably prepared. However, if a compensating pulse sequence may be implemented in place of each imperfect single-qubit rotation, then the effect of this error may be reduced. This procedure was used in Section IV to produce a concatenated CORPSE and B2 sequence robust to simultaneous amplitude and detuning errors. A similar strategy can be employed to produce accurate Ising gates in the presence of simultaneous spin-coupling (two-qubit) and amplitude (one-qubit) systematic errors [58]. Consider the control system Eq. (66) under the influence of these two independent errors. The imperfect propagator takes the form

$$V(\boldsymbol{u}(t)) = U(\boldsymbol{u}(t) + \epsilon_A \boldsymbol{\delta u}_1(t) + \epsilon_J \boldsymbol{\delta u}_2(t)) \tag{70}$$

where $\epsilon_A \boldsymbol{\delta u}_1(t) = \epsilon_A u_x(t) + \epsilon_A u_y(t)$ is the amplitude error of the single-qubit controls, and $\epsilon_J \boldsymbol{\delta u}_2(t) = \epsilon_J u_{zz}(t)$ is the error in the Ising coupling. The systematic error on the one-qubit controls $\epsilon_A \boldsymbol{\delta u}_1(t)$ complicates the synthesis of compensated Ising gates, as unitary propagators of the form Eq. (68) can no longer be reliably prepared, that is, $\mathcal{M}(\theta, \phi) = R_1^\dagger(\phi(1+\epsilon_A), 0) U_{zz}(\theta(1+\epsilon_J)) R_1(\phi(1+\epsilon_A), 0) = \mathcal{R}(\theta(1+\epsilon_J), \phi) + \mathcal{O}(\epsilon_A^2)$. This difficulty may be avoided if we use a B2 sequence to correct ϵ_A, before correcting ϵ_J using B2-J. Let $U_{B2}(\theta, \phi) = U_T \otimes \mathbb{1} + \mathcal{O}(\epsilon_A^3)$ represent the propagator produced by a B2 sequence for the target rotation $U_T = R(\theta, \phi)$ on the first qubit. The sequence B2-WJ is

$$\begin{aligned}\mathcal{M}_{\text{B2-WJ}}(\theta, 0) = {} & M_{B2}^\dagger(\phi, 0) U_{zz}(\pi(1+\epsilon_J)) M_{B2}(\phi, 0)\, M_{B2}^\dagger(3\phi, 0) U_{zz}(2\pi(1+\epsilon_J)) \\ & \times M_{B2}(3\phi, 0) M_{B2}^\dagger(\phi, 0) U_{zz}(\pi(1+\epsilon_J)) M_{B2}(\phi, 0)\, U_{zz}(\theta(1+\epsilon_J))\end{aligned} \tag{71}$$

This sequence replaces imperfect $R_1(\phi(1+\epsilon_A), 0)$ pulses with the compensated rotation produced by the B2 sequence. When $\epsilon_A = 0$, B2-WJ scales as $\mathcal{O}(\epsilon_J^3)$, and when $\epsilon_J = 0$ the sequence scales as $O(\epsilon_A^3)$. Figure 14a–c are plots of the infidelity of plain Ising pulses, and the B2-J and B2-WJ sequences in the presence of simultaneous amplitude and Ising coupling errors.

3. *Extension to* $\mathsf{SU}(2^n)$

This sequence demonstrated for two-qubits can be naturally extended to compensate operations on a network of n qubits with single-qubit operations and Ising couplings. In this case, the dynamical Lie algebra for this system is $\mathsf{SU}(2^n)$. Khaneja

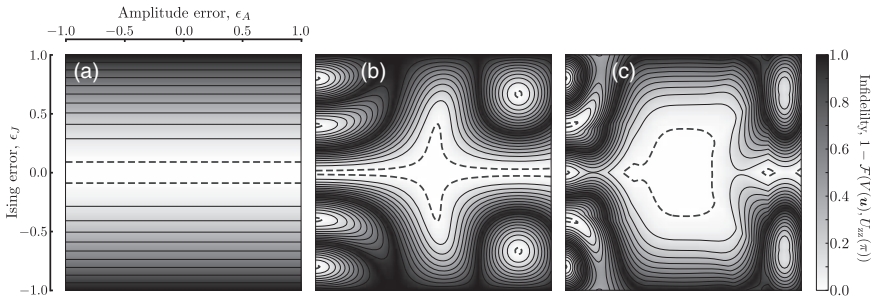

Figure 14. Infidelity of (**a**) plain Ising pulse, (**b**) B2-J, and (**c**) B2-WJ in the presence of simultaneous Ising and amplitude errors. The target rotation is $U_T = U_{ZZ}(\pi, 0)$. The dashed contour corresponds to an infidelity of 0.01, while the remaining contours are plotted at 10% intervals.

has identified a recursive Cartan decomposition for this group that allows any $U \in \mathsf{SU}(2^n)$ to be written as a product of single-qubit (local) and two-qubit (nonlocal) operations [50]. Given a pair of sequences for both single- and two-qubit operations that compensate for a particular error, it is always possible to produce a sequence for any $U \in \mathsf{SU}(2^n)$ using this decomposition. In particular, imperfect Ising gates may be replaced with a B2-J sequence, while imperfect single-qubit gates may be corrected using the methods described in Section IV. The surprising result is that one needs only a single accurate control to compensate an unlimited number of uncorrelated but systematic errors [58]. In practice, this concatenating scheme is expensive for the whole system, but it points to a method for minimizing the amount of calibration required when a few good controls can compensate nearby errors.

a. Computation on Subspaces. Several interesting proposals involve the encoding of logical qubits on subspaces of a larger Hilbert space, which may offer certain advantages over other encoding schemes. In decoherence-free subspace schemes, qubits are encoded on a subspace that is decoupled from environmental noise sources [87–89]. Also, several theoretical proposals involve the use of only two-qubit interactions to perform quantum computation [90]. In these schemes, the control algebra is chosen to be sufficiently large to allow universal computation on a subspace.

An interesting question is whether gates applied to an encoded qubit may be corrected by using a compensating sequence on the code space [58]. Recall that any gate in $\mathsf{SU}(2^n)$ may be decomposed as a product of single-qubit (encoded) and two-qubit gates; it is sufficient to consider these cases individually. We may reuse the sequences described in Section IV if the controls for the encoded gates are distorted by a similar error model. For example, given a set of two controls with correlated systematic errors $v_\mu(t) = (1 + \epsilon)u_\mu(t)$ and $v_\nu(t) = (1 + \epsilon)u_\nu(t)$, it is possible to perform compensation if the control Hamiltonians H_μ and H_ν

generate a representation of $\mathfrak{su}(2)$. In Ref. [58], it is shown that universal subspace computation can be compensated if the two-qubit Hamiltonians are of the XY model, $H = H_{xx} + H_{yy}$, but only single-qubit operations can be compensated if the two-qubit couplings are of the exchange type, $H = H_{xx} + H_{yy} + H_{zz}$.

VI. CONCLUSIONS AND PERSPECTIVES

Recent advances in quantum information and quantum control have revitalized interest in compensating composite pulse sequences. Specifically for the case of systematic control errors these techniques offer a particularly resource-efficient method for quantum error reduction. As quantum information processing experiments continue to grow in both size and complexity, these methods are expected to play an increasingly important role.

In this chapter, we have presented a unified picture of compensating sequences based on control theoretic methods and a dynamic interaction picture. Our framework allows us to view each order of the error as a path in the dynamical Lie algebra, highlighting the geometric features. Correction of the first two orders has a natural geometric interpretation: the path of errors must be closed and the signed area enclosed by the path must be zero.

The geometric method helps illuminate the construction of arbitrarily accurate composite pulses. Currently arbitrarily accurate pulse sequences are of limited use because as the length of the sequence increases, other noise sources become important. For most experiments, decoherence and random errors limit the fidelity of second-order compensation sequences. Our review of the Solovay–Kitaev pulses resulted in a modest improvement of the sequence time by implementing a new geometric construction. Shorter sequences may be achieved through numeric operation and continuous controls.

Finally, we note that CORPSE and related pulse sequences are similar to dynamically corrected gates [4], in that both remove coupling to an external field while performing an operation. Combining the methods here with the developments in dynamically corrected gates and dynamic decoupling could lead to pulse sequences robust against environmental and control errors. These operations will lower the initial error and in the end limit the resources required for quantum error correction, which will ultimately determine the feasibility of performing large quantum chemistry calculations on a quantum computer [91,92].

Acknowledgments

This work was supported by the NSF-CCI on Quantum Information for Quantum Chemistry (CHE-1037992) and by IARPA through ARO contract W911NF-10-1-0231. JTM acknowledges the support of a Georgia Tech Presidential Fellowship.

REFERENCES

1. D. Gottesman, in *Quantum Information Science and Its Contributions to Mathematics*, American Mathematical Society, 2010, pp. 15–58.
2. L. Viola, E. Knill, and S. Lloyd, *Phys. Rev. Lett.* **82**, 2417 (1999).
3. K. Khodjasteh and D. A. Lidar, *Phys. Rev. Lett.* **95**, 180501 (2005).
4. K. Khodjasteh and L. Viola, *Phys. Rev. Lett.* **102**, 080501 (2009).
5. M. H. Levitt, *Prog. Nucl. Mag. Res. Spec.* **18**, 61 (1986).
6. G. M. Huang, T. Tarn, and J. W. Clark, *J. Math. Phys.* **24**, 2608 (1983).
7. S. G. Schirmer, A. I. Solomon, and J. V. Leahy, *J. Phys. A* **35**, 4125 (2002).
8. F. Albertini and D. D'Alessandro, *IEEE T. Automat. Contr.* **48**, 1399 (2003).
9. H. Mabuchi and N. Khaneja, *Int. J. Robust Nonlin. Contr.* **15**, 647 (2005).
10. D. D'Alessandro, *Introduction to Quantum Control and Dynamics*, Chapman & Hall/CRC, Boca Raton, 2008.
11. J.-S. Li and N. Khaneja, *Phys. Rev. A* **73**, 030302 (2006).
12. J. M. Taylor et al., *Phys. Rev. B* **76**, 035315 (2007).
13. I. Chiorescu, Y. Nakamura, C. J. P. M. Harmans, and J. E. Mooij, *Science* **299**, 1869 (2003).
14. J. M. Martinis, S. Nam, J. Aumentado, K. M. Lang, and C. Urbina, *Phys. Rev. B* **67**, 094510 (2003).
15. J. Clarke and F. K. Wilhelm, *Nature* **453**, 1031 (2008).
16. D. Leibfried, R. Blatt, C. Monroe, and D. Wineland, *Rev. Mod. Phys.* **75**, 281 (2003).
17. H. Häffner, C. Roos, and R. Blatt, *Phys. Rep.* **469**, 155 (2008).
18. F. J. Dyson, *Phys. Rev.* **75**, 1736 (1949).
19. W. Magnus, *Commun. Pure Appl. Math.* **7**, 649 (1954).
20. S. Blanes, F. Casas, J. A. Oteo, and J. Ros, *Phys. Rep.* **470**, 151 (2009).
21. P. Madhu and N. Kurur, *Chem. Phys. Lett.* **418**, 235 (2006).
22. R. M. Wilcox, *J. Math. Phys.* **8**, 962 (1967).
23. F. Albertini and D. D'Alessandro, *IEEE T. Automat. Contr.* **48**, 1399 (2003).
24. M. H. Levitt and R. Freeman, *J. Magn. Reson.* **43**, 65 (1981).
25. R. Freeman, *Spin Choreography: Basic Steps in High Resolution NMR*, Oxford University Press, USA, 1998.
26. M. H. Levitt and R. Freeman, *J. Magn. Reson.* **33**, 473 (1979).
27. R. A. de Graaf, *Magn. Reson. Med.* **53**, 1297 (2005).
28. R. S. Said and J. Twamley, *Phys. Rev. A* **80**, 032303 (2009).
29. F. Schmidt-Kaler et al., *Nature* **422**, 408 (2003).
30. B. Luy, K. Kobzar, T. E. Skinner, N. Khaneja, and S. J. Glaser, *J. Magn. Reson.* **176**, 179 (2005).
31. T. Ichikawa, M. Bando, Y. Kondo, and M. Nakahara, *Phys. Rev. A* **84**, 062311 (2011).
32. L. M. K. Vandersypen and I. L. Chuang, *Rev. Mod. Phys.* **76**, 1037 (2005).
33. J. A. Jones, *Prog. Nucl. Mag. Reson. Spec.* **59**, 91 (2011).
34. S. S. Ivanov and N. V. Vitanov, *Opt. Lett.* **36**, 1275 (2011).
35. R. Gilmore, *Lie Groups, Lie Algebras, and Some of Their Applications*, Krieger Publishing Company, FL, 1994.
36. P. Brumer and M. Shapiro, *Chem. Phys. Lett.* **126**, 541 (1986).

37. M. Demiralp and H. Rabitz, *Phys. Rev. A* **47**, 809 (1993).
38. V. Ramakrishna, M. V. Salapaka, M. Dahleh, H. Rabitz, and A. Peirce, *Phys. Rev. A* **51**, 960 (1995).
39. N. Khaneja, R. Brockett, and S. J. Glaser, *Phys. Rev. A* **63**, 032308 (2001).
40. N. Khaneja, S. J. Glaser, and R. Brockett, *Phys. Rev. A* **65**, 032301 (2002).
41. D. Grensing and G. Grensing, *Z. Phys. C* **33**, 307 (1986).
42. E. B. Dykin, *Dokl. Akad. Nauk SSSR* **57**, 323 (1947).
43. D. P. Burum, *Phys. Rev. B* **24**, 3684 (1981).
44. U. Haeberlen and J. S. Waugh, *Phys. Rev.* **175**, 453 (1968).
45. J. S. Waugh, in *Encyclopedia of Magnetic Resonance*, John Wiley & Sons, Chichester, 2007.
46. H. F. Trotter, *P. Am. Math. Soc.* **10**, 545 (1959).
47. M. Suzuki, *Phys. Lett. A* **165**, 387 (1992).
48. N. Wiebe, D. Berry, P. Høyer, and B. C. Sanders, *J. Phys. A* **43**, 065203 (2010).
49. C. M. Dawson and M. A. Nielsen, *Quant. Inf. Comput.* **6**, 81 (2006).
50. N. Khaneja and S. J. Glaser, *Chem. Phys.* **267**, 11 (2001).
51. K. R. Brown, A. W. Harrow, and I. L. Chuang, Phys. Rev. A **70**, 052318 (2004); K. R. Brown, A. W. Harrow, and I. L. Chuang, Phys. Rev. A **72**, 039005 (2005).
52. S. Wimperis, *J. Magn. Reson.* **109**, 221 (1994).
53. W. G. Alway and J. A. Jones, *J. Mag. Reson.* **189**, 114 (2007).
54. J. J. L. Morton et al., *Phys. Rev. Lett.* **95**, 200501 (2005).
55. L. Xiao and J. A. Jones, *Phys. Rev. A* **73**, 032334 (2006).
56. S. E. Beavan, E. Fraval, M. J. Sellars, and J. J. Longdell, *Phys. Rev. A* **80**, 032308 (2009).
57. J. A. Jones, *Phys. Rev. A* **67**, 012317 (2003).
58. Y. Tomita, J. T. Merrill, and K. R. Brown, *New J. Phys.* **12**, 015002 (2010).
59. M. H. Levitt, *J. Chem. Phys.* **128**, 052205 (2008).
60. M. Suzuki, *Phys. Lett. A* **180**, 232 (1993).
61. R. Tycko, *Phys. Rev. Lett.* **51**, 775 (1983).
62. H. K. Cummins and J. A. Jones, *J. Magn. Reson.* **148**, 338 (2001).
63. H. K. Cummins and J. A. Jones, *New J. Phys.* **2**, 6 (2000).
64. H. K. Cummins, G. Llewellyn, and J. A. Jones, *Phys. Rev. A* **67**, 042308 (2003).
65. E. Collin et al., *Phys. Rev. Lett.* **93**, 157005 (2004).
66. M. Steffen, J. M. Martinis, and I. L. Chuang, *Phys. Rev. B* **68**, 224518 (2003).
67. L. Pryadko and P. Sengupta, *Phys. Rev. A* **78**, 032336 (2008).
68. T. E. Skinner, *J. Magn. Reson.* **163**, 8 (2003).
69. T. E. Skinner, T. O. Reiss, B. Luy, N. Khaneja, and S. J. Glaser, *J. Magn. Reson.* **167**, 68 (2004).
70. J.-S. Li, J. Ruths, T.-Y. Yu, H. Arthanari, and G. Wagner, *Proc. Natl. Acad. Sci. USA* **108**, 1879 (2011).
71. H. Geen, S. Wimperis, and R. Freeman, *J. Magn. Reson.* **85**, 620 (1989).
72. H. Geen and R. Freeman, *J. Magn. Reson.* **93**, 93 (1991).
73. N. Khaneja, T. Reiss, C. Kehlet, T. Schulte-Herbrüggen, and S. J. Glaser, *J. Magn. Reson.* **172**, 296 (2005).
74. P. de Fouquieres, S. G. Schirmer, S. J. Glaser, and I. Kuprov, *J. Magn. Reson.* **212**, 412 (2011).

75. N. Timoney et al., *Phys. Rev. A* **77**, 052334 (2008).
76. J. S. Hodges, J. C. Yang, C. Ramanathan, and D. G. Cory, *Phys. Rev. A* **78**, 010303 (2008).
77. K. Singer et al., *Rev. Mod. Phys.* **82**, 2609 (2010).
78. S. Machnes et al., *Phys. Rev. A* **84**, 022305 (2011).
79. B. Pryor and N. Khaneja, in *46th IEEE Conference on Decision and Control*, IEEE, 2007, pp. 6340–6345.
80. D. Abramovich, *J. Magn. Reson.* **105**, 30 (1993).
81. M. Steffen and R. H. Koch, *Phys. Rev. A* **75**, 062326 (2007).
82. P. Sengupta and L. Pryadko, *Phys. Rev. Lett.* **95**, 037202 (2005).
83. M. J. Testolin, C. D. Hill, C. J. Wellard, and L. C. L. Hollenberg, *Phys. Rev. A* **76**, 012302 (2007).
84. O. W. Sørensen, G. W. Eich, and M. H. Levitt, *Prog. Nucl. Mag. Res. Spec.* **16**, 163 (1983).
85. M. A. Nielsen and I. L. Chuang, *Quantum Computation and Quantum Information*, Cambridge University Press, 2000.
86. M. Lapert, Y. Zhang, S. J. Glaser, and D. Sugny, *J. Phys. B* **44**, 154014 (2011).
87. D. A. Lidar and K. B. Whaley, in *Irreversible Quantum Dynamics*, Springer, 2003.
88. Y. S. Weinstein and C. S. Hellberg, *Phys. Rev. A* **72**, 022319 (2005).
89. M. J. Storcz et al., *Phys. Rev. B* **72**, 064511 (2005).
90. A. M. Childs, D. Leung, L. Mancinska, and M. Ozols, *Quant. Inf. Comput.* **11**, 19 (2011).
91. C. R. Clark, T. S. Metodi, S. D. Gasster, and K. R. Brown, *Phys. Rev. A* **79**, 062314 (2009).
92. I. Kassal, J. D. Whitfield, A. Perdomo-Ortiz, M.-H. Yung, and A. Aspuru-Guzik, *Annu. Rev. Phys. Chem.* **62**, 185 (2011).